Journal of Materials Chemistry

www.rsc.org/materials

Volume 21 | Number 35 | 21 September 2011 | Pages 13081–13684

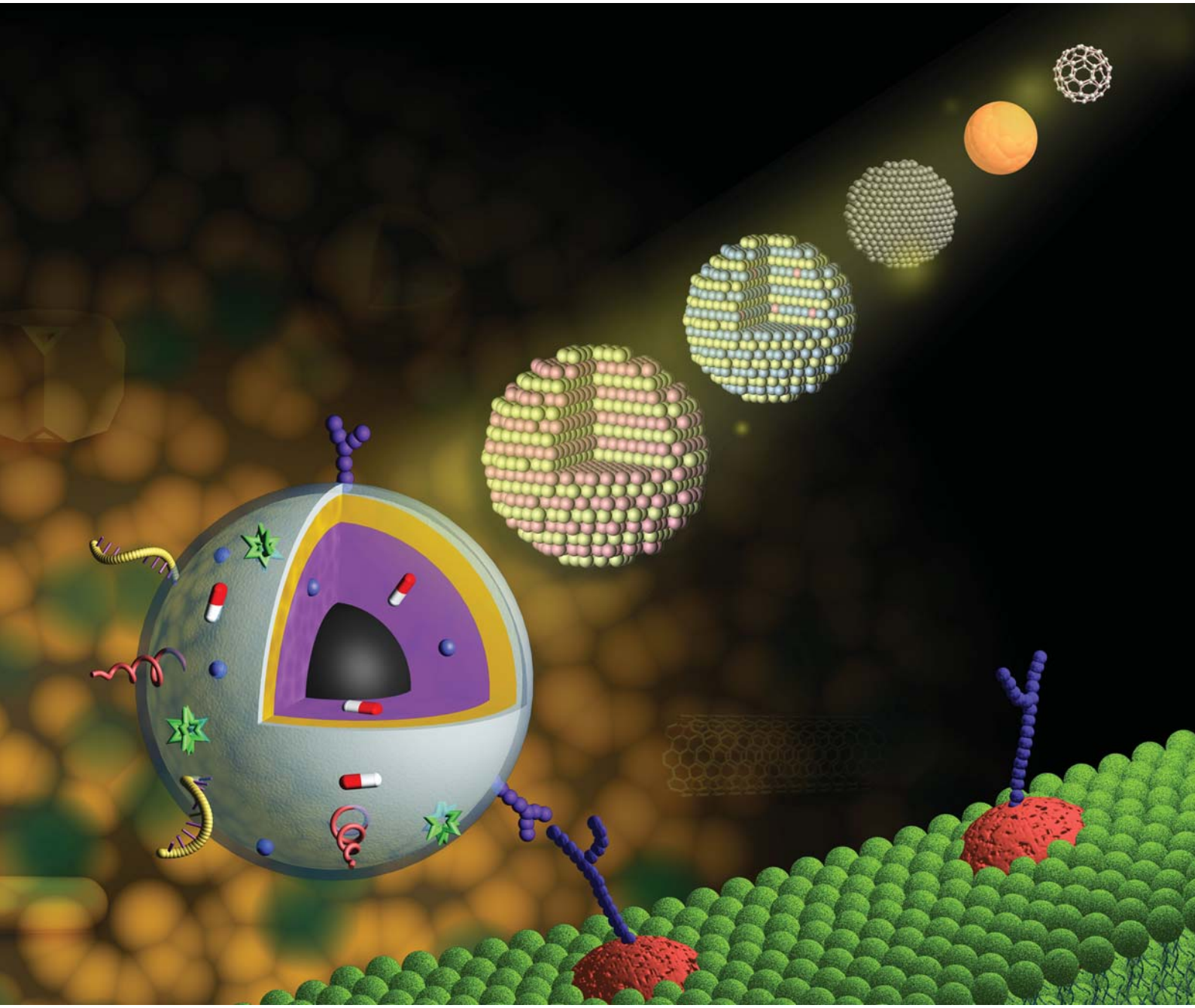

ISSN 0959-9428

RSC Publishing

FEATURE ARTICLE
Xiaogang Liu *et al.*
Emerging functional nanomaterials for therapeutics

2011 CHEMISTRY
International Year of CHEMISTRY 2011

0959-9428(2011)21:35;1-F

Journal of Materials Chemistry

Dynamic Article Links

Cite this: *J. Mater. Chem.*, 2011, **21**, 13107

www.rsc.org/materials

FEATURE ARTICLE

Emerging functional nanomaterials for therapeutics

Xuejia Xue,[a] Feng Wang[a] and Xiaogang Liu*[abc]

Received 4th April 2011, Accepted 9th May 2011
DOI: 10.1039/c1jm11401h

The recent development of functional crystalline nanomaterials for therapeutics is described. In contrast to conventional therapeutic approaches, nanomaterial-based systems present novel therapeutic opportunities; for example, by allowing active agents to be site-specifically delivered and efficiently absorbed while offering fewer or reduced side effects. In addition, nanomaterials are generally amenable to surface functionalization and interior doping. These attributes provide the nanomaterials with tunable surface, optical, magnetic, thermal and mechanical properties that are important for applications ranging from controlled release of drugs to photothermal therapy. In this article, we seek to provide a conceptual framework for understanding nanomaterial-based therapeutics. We also attempt to highlight recent therapeutic applications involving some representative nanostructured materials. With improved control over the synthesis and functional characteristics of nanomaterials, the emergence of nanomaterial-based therapeutics will likely accelerate future medical research and improve patient care.

1. Introduction

The dawn of the journey into therapeutic nanomaterials—materials that typically comprise an active ingredient together with organic or inorganic particle carriers with feature sizes of approximately 10–100 nm—can be traced back to 1950s, when Jatzkewitz reported the drug release of mescaline through a polymer–peptide–mescaline conjugate.[1] In 1995, Doxil, a liposome-based therapeutic nanomaterial containing doxorubicin, was approved by the US Food and Drug Administration for treatment of Kaposi's sarcoma.[2] With the rapid development of nanotechnology over the last decade, the exploration of functional nanomaterials for therapeutics has ramped up substantially (Fig. 1). For conventional therapeutic approaches, the dosage of drugs is difficult to optimize due to their uncontrolled

[a]*Department of Chemistry, Faculty of Science, National University of Singapore, 3 Science Drive 3, Singapore 117543. E-mail: chmlx@nus.edu.sg*
[b]*Institute of Materials Research and Engineering, Agency for Science, Technology and Research, 3 Research Link, Singapore 117602*
[c]*Advanced Materials for Micro-and Nano-Systems Program, Singapore-MIT Alliance, Singapore 117576*

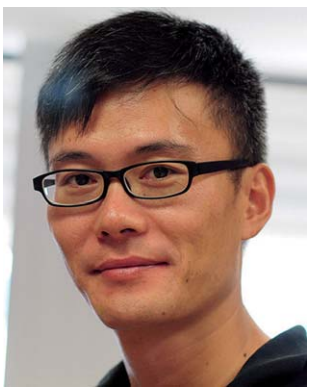

Xuejia Xue

Xuejia Xue was born in Jiangsu, China. He received his BSc (1998) degree in Polymer Science and Engineering from Nanjing University and ME (2004) degree in Chemistry and Chemical Engineering from Southeast University. He is currently pursuing a PhD degree under the supervision of Prof. Xiaogang Liu in the Department of Chemistry at National University of Singapore. His PhD thesis focuses on the rational design and fabrication of functional nanomaterials with unique optical properties for detection of metal ions and biological macromolecules.

Feng Wang

Feng Wang was born in Shaanxi, China. He obtained his BE (2001) and PhD (2006) degrees in Materials Science and Engineering from Zhejiang University. His PhD thesis was focused on the synthesis and characterization of lanthanide-doped fluoride nanomaterials under the supervision of Profs. Mingquan Wang and Xianping Fan. He joined the group of Prof. Xiaogang Liu at the National University of Singapore in 2007. His current research focuses on the synthesis, spectroscopic investigation and application of luminescent nanomaterials.

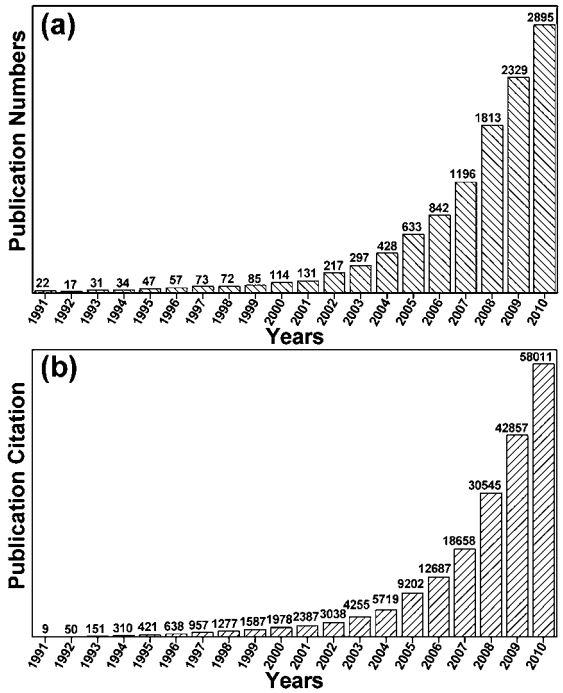

Fig. 1 Research interests on nanomaterial-based therapeutics over the past twenty years as indicated by (a) publication numbers and (b) publication citations, respectively. The data are generated through the Web of Science database with keyword search of nano* and therap*.

delivery, slow onset of action, undesirable side effects, and the unpredictable medication break-down associated with digestive enzymes. In contrast, the use of therapeutic nanomaterials has enabled new mechanisms for controlling the delivery of drugs and has enhanced the effectiveness of drugs, while significantly minimizing side effects.[3–8] Owing to their small dimension, nanomaterials can be taken much faster across cell membranes. They are also amenable to surface modification and functionalization with ligand molecules to promote targeting to specific diseased cells or tissues.

In addition to their prominent role as a means to drug delivery, functional nanomaterials have shown promise as direct modalities for treatment of common diseases such as cancers, abnormal blood vessel growth, infectious diseases and tissues. For example, fullerenes that consist of a spherical arrangement of dozens of carbon atoms have shown neuroprotective effects against neurodegenerative diseases.[9] Magnetic nanoparticles and carbon nanotubes have also been used to function directly as therapeutic materials for killing cancerous and precancerous cells by thermal ablation through use of an external stimulus.[10] Interestingly, polymer-coated quantum dots, which are toxic to cells on ultraviolet (UV) irradiation, have shown potential use as photosensitizers for photodynamic therapy.[11] The cytotoxicity of quantum dots, induced by the generation of reactive oxygen species, can be harnessed as a comparatively non-invasive means of killing cancer cells. Recent advances in the synthesis of lanthanide-doped upconversion nanocrystals have provided a novel class of therapeutic nanomaterials for photodynamic therapy.[12] These luminescent nanomaterials can convert near-infrared (NIR) light into visible light and allow targeted treatment of cancer cells profiled at substantial depth as the NIR irradiation penetrates deep into biological tissues.

In this article, we discuss several substantial topics of current interest in the area of therapeutic nanomaterials involving using crystalline nanomaterials as drug carriers or direct therapeutic modalities. Rather than attempting to provide a complete historical survey, our emphasis here is on identifying developing areas of research. These range from rational design of therapeutic nanomaterials for enhanced permeability and targeted drug delivery to the investigation of novel nanomaterials for relatively unexplored therapeutic applications (*e.g.*, upconversion nanoparticle-based therapy). Although an enormous amount of research is ongoing in this area, we focus our attention on nanomaterials that can be affected by external stimulation. These include metallic and magnetic nanoparticles, quantum dots, upconversion nanoparticles and carbon-based nanomaterials. Although most will not be quickly translated into practical applications in clinic settings because of their own toxicity risks, our efforts here are to highlight the ability to use fundamental chemical principles to design and prepare functional nanomaterials displaying exciting therapeutic effects.

2. Rational design of therapeutic nanomaterials

Nanomaterial characteristics, such as size, shape, composition and surface properties, are fundamental issues that ultimately influence the therapeutic effect of a drug. In principle, therapeutic nanomaterials can be broadly classified into two groups. The first group refers to small drug molecules or biological substances that self-assemble into micelle-like nanoparticles possessing a dual function as drug carriers. The second group is primarily based on hybrid nanomaterials with therapeutic molecules either bound to the surface of nanomaterial carriers or encapsulated by the carriers. The carriers could either have more

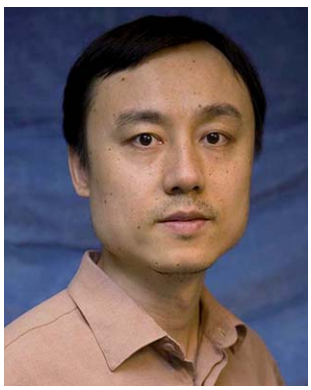

Xiaogang Liu

Xiaogang Liu was born in Jiangxi, China. He earned his BE degree (1996) in Chemical Engineering from Beijing Technology and Business University. He received his MS degree (1999) in Chemistry from East Carolina University under the direction of Prof. John Sibert and completed his PhD (2004) at Northwestern University under the supervision of Prof. Chad Mirkin. He then became a postdoctoral fellow in the group of Prof. Francesco Stellacci at MIT. He joined the faculty of the National University of Singapore in 2006. He holds a joint appointment with the Institute of Materials Research and Engineering, Agency for Science, Technology and Research. His interests include nanomaterials synthesis, supramolecular chemistry and surface science for catalysis, sensors and biomedical applications.

substances of an organic nature, such as stimulus-responsive polymers, or comprise inorganic crystalline structures. The latter therapeutic design can harness the unique optical and magnetic properties, provided by the inorganic nanomaterials, for controlled and targeted drug delivery.

2.1 Nanomaterial size and shape

The size of therapeutic nanomaterials is perhaps the most significant parameter that dictates the efficacy of drug delivery. Notably, the manipulation of particle size can exert control over the bio-distribution and pharmacokinetics of drug molecules within the body following systemic administration. A metal nanoparticle of about 20 nm has a ratio of surface area to mass much larger than that of the bulk material. This property enables the nanoparticle to efficiently bind, absorb and carry multiple types of compounds such as drug molecules, probes and proteins. In addition, small nanoparticles exhibit high level of accumulation at tumor sites and access to places where large particles cannot reach.[16] Thus, nanoparticles can be controlled to provide long or short circulation times within the bloodstream by controlling particle size and surface properties. Experiments from animal models suggest that sub-150 nm, neutral or slightly negatively charged entities can move through tumor tissue. For effective cancer therapy, it is generally thought that the size of therapeutic nanomaterials should be in the range of 10–100 nm, as larger particles have limited diffusion in the extracellular space.[17] For instance, an *in vivo* study on live mice revealed an upper uptake threshold of 100 nm particles when dosed into the circulatory system.[18] However, larger particles were mostly trapped in lymphoid tissues of the stomach.[18]

It should be noted that the ability to remove nanomaterials by biological organs or systems strongly depends on the size of the nanomaterials. The removal of the nanomaterials after a therapeutic process is particularly important as the accumulation of residual particles may impose hazardous risks to the patient. For example, iron poisoning with hepatic injury has been the subject of attention for a half-century.[19] The liver and gastrointestinal tract are the two main targets of iron intoxication. Studies have shown that particles smaller than 5.5 nm can be removed with relative ease by the body's excretory system.[20]

For optical nanomaterials used as direct therapeutic tools, the control of particle size is essential as different sized nanoparticles have radically different optical properties (Fig. 2). Also, plasmonic metal nanoparticles have optical properties that are highly sensitive to particle shape.[21] One can manipulate the shape of metal nanoparticles as a result for particular therapeutic applications that require a specific wavelength of light.

Non-spherical particles with rough edges and irregular surfaces typically have more surface area than spherical particles with smooth surfaces. The surface area can affect the binding capacity of the particles to cancerous cells and tissues. Thus, the design of non-spherical particles can extend the particle's residence times *in vivo*. Needle-like carbon nanotubes have several advantages over spherical nanoparticles for drug delivery, including superior flow dynamics, enhanced ability to penetrate cellular membranes and increased capacity to carry multiple types of drugs at high density.

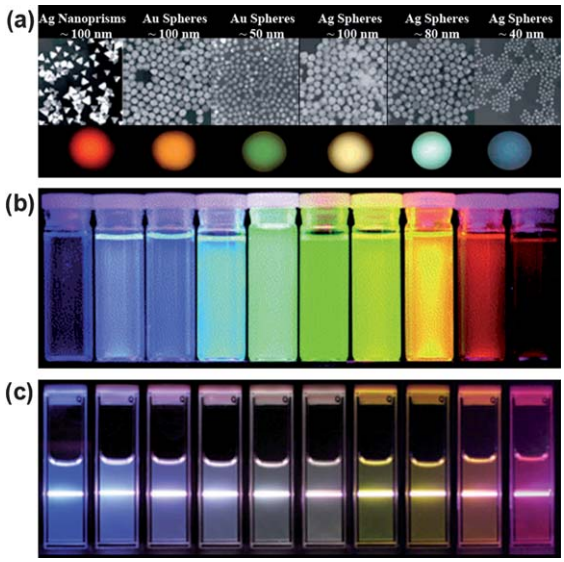

Fig. 2 Multicolor fine-tuning of nanomaterials. (a) The light-scattering properties of noble metal nanoparticles with varied sizes and shapes. (b) The size-dependent emission of quantum dots. (c) A series of lanthanide-doped nanoparticles with tunable upconversion emissions. (Reprinted with permission from: (a) ref. 13, (b) ref. 14 and (c) ref. 15. Copyright 2001, 2001, 2008, respectively, the American Association for the Advancement of Science, Nature Publishing Group and American Chemical Society.)

2.2 Nanomaterial composition

Therapeutic crystalline nanomaterials currently under investigation typically comprise gold nanoparticles with varied shapes, magnetic nanoparticles, carbon-based nanomaterials, quantum dots and lanthanide-doped upconversion nanoparticles (Fig. 3). The therapeutic effect and potential toxicity risks are closely related to materials composition. Different chemical composition imparts the nanomaterials with specific optical, electrical and magnetic properties, which are highly relevant towards particular therapeutic applications.

The surface reactivity of nanoparticles is dependent on their chemical composition, which in turn controls particle circulation time, the interaction of nanoparticles with their local environment, and ultimately the efficiency of receptor targeting. Importantly, the cytotoxity of nanoparticles can be roughly estimated by their chemical composition. For instance, polymeric nanoparticles are more biocompatible and less toxic than crystalline inorganic nanoparticles. Among inorganic nanoparticles, silica-based nanoparticles are perhaps the most biocompatible nanomaterials, and are frequently used as drug

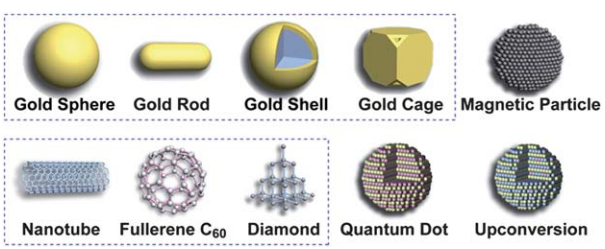

Fig. 3 Summary of different classes of therapeutic nanomaterials discussed in this article.

carriers for therapeutics. Quantum dots containing heavy metals such as cadmium and lead are substantially more toxic than metallic and lanthanide-doped nanoparticles.

2.3 Nanomaterial crystallinity

The crystallinity of nanomaterials is particularly important for their applications in photodynamic therapies where strong light emissions from the nanomaterials are required. For instance, hexagonal phase sodium yttrium fluoride ($NaYF_4$) offers about an order-of-magnitude enhancement of upconversion efficiency relative to its cubic phase counterpart.[22] Indeed, recent applications of $NaYF_4$ nanomaterials in photodynamic therapy are almost exclusively based on hexagonal phase $NaYF_4$ nanoparticles. Carbon nanotubes and fullerenes, which share same chemical characteristics, have considerably different surface reactivity. The introduction of structural defects to crystalline nanomaterials also imparts a high surface reactivity to cancer cells and tissues.

2.4 Nanomaterial functionalization

Although some nanomaterials have excellent intrinsic therapeutic properties, they generally do not have suitable properties for targeted *in vivo* applications. Nanomaterial functionalization through surface engineering or interior modification is thus essential. These methods include coating of biocompatible polymer, conjugation with target-specific agents, fluorescent probes as well as cell-membrane penetration ligands, functionalization with a magnetic core, and doping with luminescent lanthanide ions (Fig. 4). For example, gold nanoparticles can be made water-soluble by attaching appropriate thiolated DNA molecules to the particle surface. Another important aspect of surface modification is to render the nanomaterials chemical inert and biocompatible. A variety of biocompatible hydrophilic polymers, including poly(ethylene glycol), chitosan, polyethyleneimines and polysaccharides, have been reported as the coating materials.[23–26] In principle, the composition and thickness of the shell coatings are determined by the surface structure of the core materials. Silica, a known nontoxic item, can be readily coated onto quantum dots with controllable thickness.[27] The coating of quantum dots with a thin layer of silica shell, not only imparts improved colloidal stability and biocompatibility, but also provides substantial protection of the core particles.

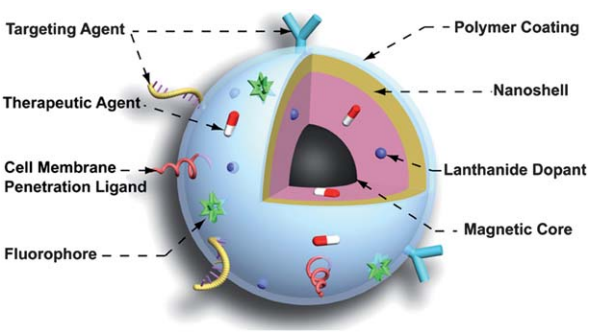

Fig. 4 Nanomaterial functionalization through surface engineering or interior modification for targeted delivery of therapeutic agents.

Surface modification provides nanomaterials with a highly structured surface so that a specific targeting ligand can be developed, allowing it to be used in targeted drug delivery. This delivery route is particularly attractive for pharmaceutical compounds which are hardly soluble *in vivo*. These nanomaterials also offer much greater specificity than conventional therapeutic drugs by actively binding to receptors located primarily in the walls of diseased cells or tissues. The targeting ligand can enhance the retention of the nanomaterials to the target tissue and also mediate the uptake or ingestion of the nanomaterials by a target cell type.

The integration of a magnetic element into the nanomaterials may allow for therapeutic agents to be concentrated locally or allow possible implementation of interactive control for improved targeting efficiency. In addition, fluorescent molecules and lanthanide ions could be incorporated for tracking physiological events taking place *in vivo* and for assessing the target interaction and modulation in the diseased cells and tissue.

2.5 Delivery routes and therapeutics

Nanomaterial-mediated therapeutic processes typically involve three major steps: (i) delivery of nanostructured carriers directly into cancer sites or into the blood stream, (ii) adsorption and uptake of the nanomaterials by cancer cells, and (iii) delivering therapeutics either through the anticancer payload or directly through the nanomaterials by using external energy sources such as optics or magnetics.

The choice of a specific delivery route, driven by a number of considerations with regard to patient acceptability, the surface properties of the materials and cost effectiveness, is the fundamental aim of researchers working in the field. Recent technological advances have allowed the development of a diversity of delivery routes, including peroral uptake, topical application, pulmonary delivery and parenteral injection.

Among various routes of therapeutic delivery, the peroral route directly through the mouth represents the most intensively investigated mode of administration as it offers advantages of convenience and non-invasiveness. However, the effectiveness of this approach is often hampered by the interference of digestive enzymes and non-specific adsorption in the lymphoid tissues.[28] Topical application through the skin is another non-invasive technique that provides localized delivery and avoids the risks and inconveniences of parenteral injection. Limitations of topical application include poor permeability of some nanomaterials, lack of dosage precision and possibility of allergenic reactions.[29] Pulmonary delivery through inhalation represents an attractive, rapid and patient-friendly route for drug administration. The lungs provide a rich blood supply and enormous surface area (up to 100 m^2) for drug adsorption and the non-invasive nature of pulmonary delivery has the potential to greatly improve patient quality of life. However, pulmonary delivery can be complicated by safety concerns and the effect of disposition exerted by the respiration process.[30] Parenteral injection is given through the veins of the circulatory system rather than through the digestive system. The parenteral route can introduce nanomaterials into the body through intravenous, intramuscular, subcutaneous injection for a rapid adsorption.[31]

Once administered into the blood, nanostructured carriers are circulated through the blood stream. It should be noted that nanomaterials smaller than the renal filtration threshold are able to be cleared rapidly from the body *via* renal filtration and urinary excretion. Although nanomaterial toxicity would be minimized through this process, the therapeutic utility of nanomaterials could be substantially affected. Many therapeutic nanomaterials access cancer cells through endocytosis.[32] Endocytosis is a process by which the cells absorb the nanomaterials by engulfing them. In addition to endocytosis, another major mechanism of nanomaterial uptake by cancer cells is through the enhanced permeability and retention (EPR) effect.[33] The EPR effect occurs in tumors with ill-formed or disrupted blood vessels. The EPR effect allows nanomaterials to pass from the blood vessels and accumulate into cancer sites. However, it is possible that small sized nanoparticles would traverse freely back into the blood stream as a result of diffusion due to high particle concentrations in the cancer sites after an extended period. For targeted nanomaterial delivery systems, a ligand or an antibody can be attached to the nanomaterials prior to injection. The antibody aids the recognition of the antigens that are expressed by the malignant cells at different stages, resulting in improved accumulation of the nanomaterials into the cancer sites.

The key benefit of using crystalline optical and magnetic nanomaterials is the ability to precisely control the delivery of therapeutics by external stimulus manipulation. Various schemes of therapeutics through use of these nanomaterials are summarized in Fig. 5. For example, NIR absorbing nanoparticles shows great promise for selective, minimally invasive photo-thermal tumor ablation. Another notable example is lanthanide-doped upconversion nanoparticles that have shown potential in photodynamic therapy. Upconversion nanoparticles readily convert low energy NIR light into the visible range. The upconverted light subsequently excites specific photosensitizers, leading to the generation of reactive oxygen species for treatment of deep-lying tumors.

3. Noble metal nanomaterials

Noble metal nanomaterials exhibit a characteristic optical property known as the surface plasmon resonance. Surface plasmons are coherent electron oscillations that are induced by the interaction between the conduction band electrons of metal nanoparticles and an electromagnetic field in form of light. The frequency and magnitude of surface plasmon waves depend on the size, shape and dielectric constant of the metal nanomaterials as well as the refractive indices of the media that the electromagnetic field wave interacts with along its propagation path. Importantly, the absorbed light by the nanomaterials can be converted into thermal energy, which can be further explored to generate a localized increase in temperature in the vicinity of targeted cells. This property, combined with high biocompatibility of noble metal nanomaterials, provides a platform for potential biological applications in plasmon-induced drug delivery or photothermal therapy.

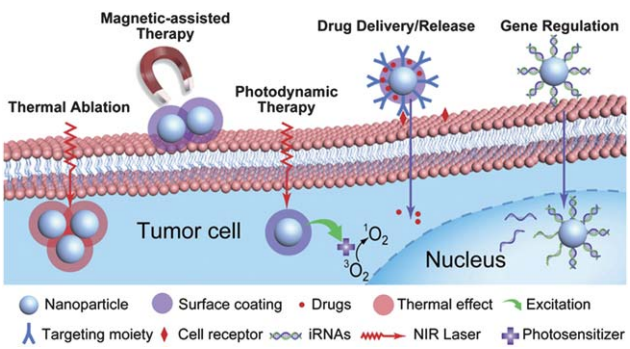

Fig. 5 Various schemes of therapeutics including thermal ablation, magnetic-assisted therapy, photodynamic therapy, drug delivery/release, gene regulation.

Among noble metal nanomaterials, gold nanomaterials have been most extensively investigated for therapeutic applications due to their excellent oxidation resistance and simple synthetic procedure. Another attractive aspect of using gold nanomaterials is that, with a facile ligand-exchange step, one can modify the nanomaterials with readily available DNA interconnect molecules. DNA molecules can be prepared and functionalized with ligands or antibodies for diagnostic tests as well as targeted delivery of a potent cancer drug. Furthermore, gold nanomaterials offer size-dependent tunable optical absorption typically in the visible spectral region, and by adjusting the shape and structure of the nanomaterials, the optical absorption can be extended to the NIR region for maximal tissue penetration. Gold nanomaterial-based approaches offer high level of plasmonic heating at a target site, which are four to five orders of magnitude greater than those of conventional photoabsorbing dyes.[34] In this section, selected examples of gold nanomaterials with different morphologies and structures are highlighted in photo-mediated therapeutic studies (Table 1).

3.1 Spherical nanoparticles

Gold nanoparticles can be readily prepared on a relatively large scale by using two commercially available starting materials, hydrogen tetrachloroaurate and sodium citrate.[52] Upon surface conjugation of DNA molecules,[21,53–63] gold nanoparticles can be stored at room temperature without aggregation for several months. In contrast to other types of gold nanostructures, gold nanoparticles can be made with a high degree of monodispersity and small feature size that promotes their entry into cells through endocytosis. In addition, gold nanoparticles with size less than 20 nm are susceptible to biodegradation, which results in a short circulation time in biological systems.[64] The short circulation process of gold nanoparticles may reduce the risks for patients suffering from side effects. However, gold nanoparticles have optical absorption typically located in the visible spectral region, which limits their applications for treatment of deep-lying cancer and tumors.

Thermal ablation. As one of the most promising advances in therapeutics, thermal ablation treats cancer tumors by heat-generating probes directly injected into the malignant tissue under investigation. This method allows surgeons to treat tumors with minimal damage to surrounding tissue as cancer cells are more susceptible to destruction by heat than normal tissue cells. For cancers that are often difficult to treat surgically, thermal ablation offers a better alternative to eliminate or shrink tumors.

Table 1 Selected gold nanomaterials used for therapeutic applications[a]

Shape and size	Therapeutic mechanism	Therapeutic target	Experimental condition	Ref.
Nanospheres (~20 nm)	Thermal ablation of cells through use of NIR-irradiated Au sphere aggregates	*T. gondii* tachyzoites	*In vitro*	35
Nanospheres (~50 nm)	Thermal damage of cell membranes *via* photothermal vapor nanobubbles	Lung carcinoma cells (A549)	*In vitro*	36
Nanospheres (~27 nm)	Drug delivery through a hydrophobic cyclodextrin shell for intracellular uptake	A549 cells and MCF-7	*In vitro*	37
Nanospheres (~13 nm)	Platinum drug delivery through oligonucleotide-modified Au nanoparticles for cell uptake	U2OS, A549, HeLa and PC3 cells	*In vitro*	38
Nanospheres (~13 nm)	Gene delivery through siRNA-modified Au nanoparticles	HeLa cells	*In vitro*	39
Nanospheres (~2 nm)	Superficial radiation therapy	Bovine aortic endothelial cells	*In vitro*	40
Nanospheres (~50 nm)	Ligand-mediated therapy	Neuro2A cells in organs of mice	*In vivo*	41
Nanorods (~60 nm; AR: ~3.9)	Thermal ablation of tumor cells	HOC 313 clone 8 and HSC 3 cells	*In vitro*	42
Nanorods (~60 nm; AR: ~4.0)	Laser-assisted thermal activation	The porcine anterior lens capsule	*Ex vivo*	43
Nanorods (~44, 89 nm; AR: ~4.0, 5.4)	Controlled release of oligonucleotides *via* dual-mode laser irradiation	—	*In vitro*	44
Nanorods (~47 nm; AR: ~3.6)	Controlled release of drugs through light-mediated thermal activation	MDA-MB-435 tumor in mice	*In vivo*	45
Nanoshells (core: ~138 nm; shell: ~37 nm)	Reflectance-based probes for tumor imaging	Breast cancer cells: SK-BR-3, HCC-1419, JIMT-1	*Ex vivo*	46
Nanoshells (core: ~127 nm; shell: ~6 nm)	Controlled release of drugs triggered by Au shell heating	-	*In vitro*	47
Nanocages (~40 nm)	Drug release and thermal ablation through NIR light irradiation	MDA-MB-231 cells	*In vitro*	48
Nanocubes (~45 nm)	Cell imaging	Liver cancer cells (QGY), embryo kidney cells (293T)	*In vitro*	49
Hollow nanospheres (~30 nm)	Photothermal ablation therapy	Human squamous carcinoma A431 cells	*In vivo* and *in vitro*	50
Hollow nanospheres (~43.5 nm; shell: ~3–4 nm)	Photothermal ablation therapy	B16/F10 cells	*In vivo*	51

[a] AR: Aspect ratio.

Kim and co-workers[64] have recently reported pH-induced aggregation of gold nanoparticles in mild acidic intracellular environments. With a relatively small size of 10 nm and a hydrolysis-susceptible surface, these nanoparticles could be internalized into cancerous cells and accumulated to form aggregates. On NIR excitation at different intensities, the particle aggregates were shown to efficiently destroy cancer cells (Fig. 6). Pissuwan *et al.*[35] have also demonstrated the utilization of plasmonic heating for destroying *T. gondii*, a pathogenic parasite. They showed that destruction of *T. gondii* can be simply achieved with photoirradiation of antibody-functionalized gold nanoparticles of approximately 20 nm in diameter.

Drug carriers. Gold nanoparticles are ideal drug carriers that are able to precisely tune the release rate of the drugs attached to the particles. The kinetic control over drug release is critical for successful therapeutics. In some clinical studies, the efficacy of drugs is shown to be enhanced through a slow release process and prolonged exposure at a given dose. However, there are clinical cases of good therapeutic effects associated with a rapid release of drugs at high concentrations. Additionally, gold nanoparticles of 20–50 nm in sizes are sufficiently large to accommodate multiple types of drug molecules. Parallel therapeutic applications can be simultaneously carried out with a nanoparticle in a controlled manner. An interesting demonstration by Rotello and co-workers[65] showed that photocontrolled release of a caged anticancer drug (5-fluorouracil) can be achieved by using a gold nanoparticle carrier. The drug molecule is covalently attached to a 10-nm gold nanoparticle with a nitrobenzyl anchoring group (Fig. 7a). Upon UV irradiation, the nitrobenzyl group underwent photolytic cleavage accompanied by the release of the drug molecule. The drug release process was confirmed through cell culture studies with the drug-loaded nanoparticles. Optical micrographs showed the change in cell morphology after incubation of the nanoparticles with the cells for 96 h (Fig. 7b and d). Fluorescence-microscopy images revealed the suppression of cell viability, indicating the successful delivery of the anticancer drugs (Fig. 7c and e). Other different systems of drug delivery

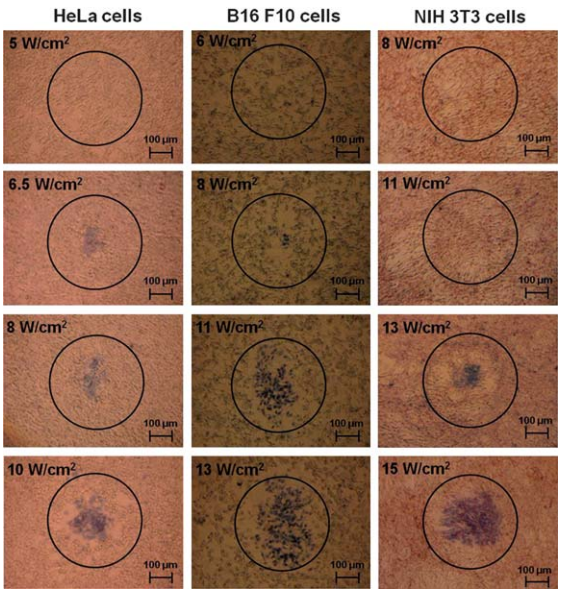

Fig. 6 Thermal ablation of HeLa, B16F10, NIH 3T3 cells using gold nanoparticle aggregates under different laser power intensities. The marked circles indicate the position of laser spot. (Reprinted with permission from ref. 64. Copyright 2009, American Chemical Society.)

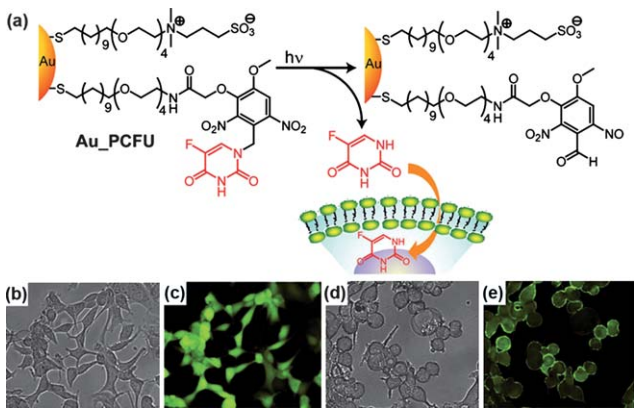

Fig. 7 Photoregulated release of anticancer drugs. (a) Scheme showing the photochemical reaction of 5-fluorouracil attached to a gold nanoparticle. (b, c) Bright-field and fluorescence-microscopy images of the cells stained with calcein AM dye. (d, e) corresponding bright-field and fluorescence-microscopy images of the cells treated with the drug-loaded nanoparticles. (Reprinted with permission from ref. 65. Copyright 2009, American Chemical Society.)

through use of gold nanoparticle carriers have been put to the test by the groups of Mirkin, Mukherjee, Kim and Gong.[37,38,66,67]

Gene therapy and regulation. DNA-modified gold nanoparticles show resistance to cell nuclease degradation and high cellular uptake. Owing to their enhanced binding properties, DNA-modified gold nanoparticles have recently been used for antisense gene control and detection of intracellular RNA. However, it is challenging to load and transport RNA across cell membranes by utilizing polyvalent particles, as RNA is generally less stable than DNA. By using polyvalent RNA–gold nanoparticle conjugates, Mirkin and co-workers[68] have demonstrated

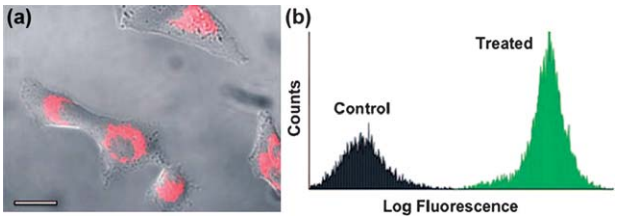

Fig. 8 Cellular uptake of RNA–gold nanoparticle conjugates. (a) Fluorescence microscopy images of HeLa cells incubated for 6 h with the conjugates (cyanine 5-labeled RNA). Scale bar is 20 μm. (b) Flow cytometry comparative analysis of nanoparticle-treated cells and untreated controls. (Reprinted with permission from ref. 68. Copyright 2009, American Chemical Society.)

effective gene regulation in the context of RNA interference. The as-prepared gold nanoparticles were introduced into HeLa cells without the need of transfection agents. Confocal imaging studies revealed fluorescence throughout the cells after treated with the nanoparticles for 6 h (Fig. 8a). Flow cytometry also confirmed internalization of the nanoparticles in greater than 99% of the cell population (Fig. 8b).

DNA damaging. Despite their enormous utility as drug carriers, gold nanoparticles have shown to directly disrupt regulated cell cycle, thereby causing DNA damage in cancer cells. As a demonstration of this concept, Kang *et al.*[69] reported peptide–gold nanoparticle conjugates that selectively target the nucleus in cancer cell. In their design, two types of peptides, arginine–glycine–aspartic acid and nuclear localization signal peptides, were used to provide cancer cell surface- and nucleus-specific targeting, respectively. In the presence of the nanoparticles, cytokinesis arrest was observed by dark-field imaging of living cells in real time, followed by binucleate cell formation (Fig. 9). However, for untreated cells and cells with nanoparticles present in the cytoplasm, no disruption of cell cycle was observed. The efficient disruption of the cell cycle was evident due to the preferential attachment of the peptide–gold nanoparticle conjugates to the cell nucleus.

Cell-membrane penetration. Nanoparticle penetration into cell membranes without bilayer disruption is important for efficient therapeutics. Nanoparticles are typically internalized into cells by passing cell plasma membranes through endocytosis.

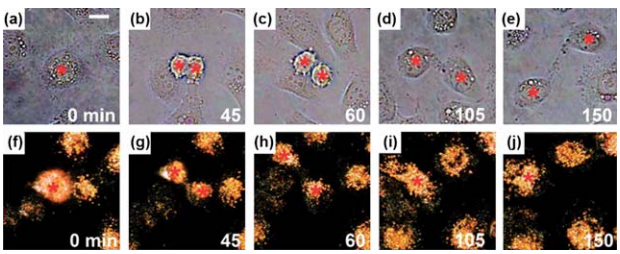

Fig. 9 Real-time images of cancer cell division showing an apparent cytokinesis arrest (h) followed by binucleate cell formation (i, j) in the presence of 0.4 nM nuclear-targeting gold nanoparticles. This phenomenon was not observed in controls without particle incubation (a–e). Red stars indicate the nuclei. Scale bar: 10 μm. (Reprinted with permission from ref. 69. Copyright 2009, American Chemical Society.)

However, unlike cell-membrane penetration by some biomacromolecules (*e.g.*, cell-penetrating peptides), the membrane penetration by nanoparticles often induces overt lipid bilayer disruption.[70] Membrane disruption is a toxic effect that hampers the use of the nanoparticles for drug delivery. Indeed, controlling the balance between the level of penetration and potential risk of membrane disruption is one of the key challenges in designing therapeutic nanomaterials. Stellacci and co-workers[70] have recently presented an innovative strategy for delivering nanoparticles into the cellular cytoplasm without bilayer disruption. Inspired by the ordered amphiphilic structure of some cell-penetrating peptides, they modified gold nanoparticles of ~6 nm with a shell of alternating hydrophobic and hydrophilic ligands. Investigation by scanning tunneling microscopy showed that these ligands are regularly arranged in ribbon-like domains of alternating composition (Fig. 10a). Importantly, the rippled particles were able to penetrate cell membranes at 37 and 4 °C without notable evidence of membrane disruption. In stark contrast, particles with identical hydrophobic content only exhibited moderate cell-penetrating abilities.

3.2 Nanorods

In contrast to spherical gold nanoparticles, gold nanorods exhibit a characteristic longitudinal surface plasmon in addition to a transverse surface plasmon. The longitudinal surface plasmon provides a much larger extinction coefficient than the transverse mode due to oscillation of electrons in the long direction of the nanorod. Consequently, gold nanorods exhibit strong extinction peaks in the upper visible or NIR parts of the spectrum. By tailoring the aspect ratio of the rods, one can readily tune the position of the extinction peak (Fig. 11a). Gold nanorods with aspect ratios of between 3 and 4 exhibit optical absorption spectra with peak maxima that fall between 700 and 900 nm, the so-called "medical spectral window[71] (or tissue window)" associated with minimum absorption of light in most human tissues (Fig. 11b).

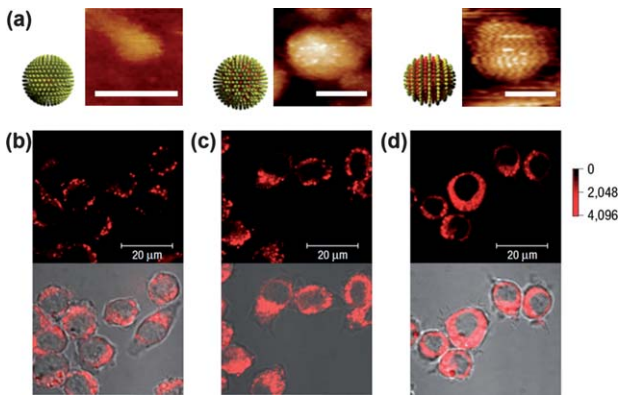

Fig. 10 Cell-membrane penetration through use of rippled nanoparticles coated with a binary hydrophilic and hydrophobic thiolated molecules. (a) Schematic diagrams of the ligand shell structure of the nanoparticles and corresponding scanning tunneling microscopy images (scale bars are 5 nm). (b–d) Upper panels: fluorescence images with an intensity scale bar. Lower panels: brightfield/fluorescence overlay images of dendritic cells incubated with (b) 11-mercapto-1-undecanesulfonate (MUS); (c) a binary mixture of MUS and 1-octanethiol; and (d) the nanoparticles modified with MUS and 1-octanethiol for 3 h in serum-free medium at 37 °C. (Reprinted with permission from ref. 70. Copyright 2008, Nature Publishing Group.)

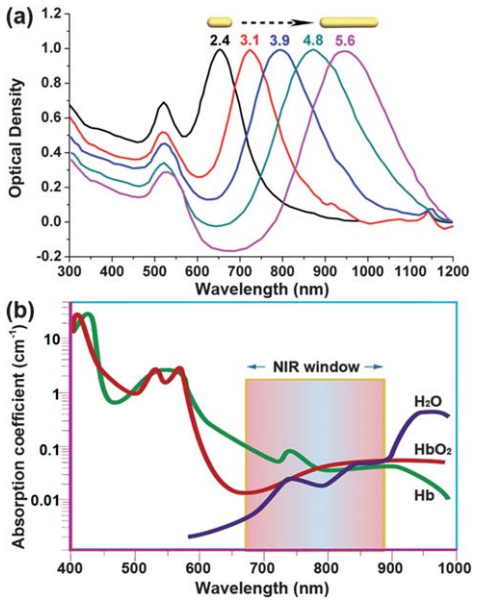

Fig. 11 Tuning surface plasmon resonance of gold nanorods into NIR window. (a) Absorption spectra of gold nanorods with aspect ratios ranging from 2.4 to 5.6. (b) Absorption spectra of deoxy-hemoglobin (Hb), oxyhemoglobin (HbO_2) and water. (Reprinted with permission from (a) ref. 42 and (b) ref. 71. Copyright 2006 and 2001, respectively, American Chemical Society and Nature Publishing Group.)

EI-Sayed and colleagues[42] have pioneered the application of nanorods for photothermal therapy. In their work, the nanorods were conjugated to anti-epidermal growth factor receptor (anti-EGFR) and then incubated with one nonmalignant epithelial cell line (HaCaT) and two malignant epithelial cell lines (HOC313 clone8 and HSC3) for 30 min at room temperature. The cell solutions were exposed to the NIR laser irradiation and subsequently stained with trypan blue for cell viability test. They found that the malignant cells were destroyed at about half the laser fluence needed for destroying nonmalignant cells. In a more recent demonstration of using gold–silver hybrid nanorods, Tan and co-workers[72] showed that aptamer-conjugated nanorods can target specific tumor cells. Following laser irradiation at 808 nm, about 50% of the target cells were destroyed at a laser power of 600 mW.

The use of multifunctional gold nanorods for drug and gene delivery has also been reported. For example, Chakravarthy *et al.*[73] have recently reported nanorod-mediated delivery of single-stranded RNA (ssRNA) for treatment of seasonal and pandemic flu. The nanorods were functionalized with 5′PPP-ssRNA to form biocompatible nanoplexes. They observed that the binding of an ionic RNA to cationic nanorods reduced overall charge of the nanoplex, thereby enabling increased uptake of the nanoplex into the target cell.

3.3 Nanoshells

Gold nanoshells have also shown prospects as tunable plasmonic absorbers. Zhang and co-workers[50,51,74,75] have shown that the plasmon resonance and peak absorption efficiency in nanoshells

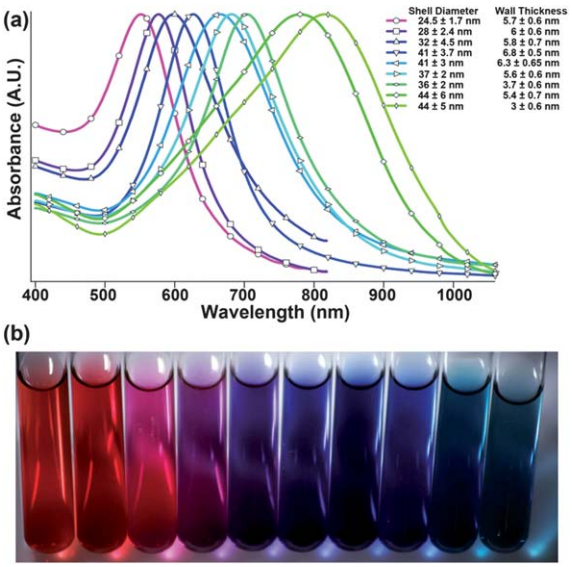

Fig. 12 (a) UV-visible absorption spectra of nine hollow gold nanoparticle (HGN) samples with varying diameters and wall thicknesses. (b) Image showing color range of HGN solutions. The vial on far left contains solid gold nanoparticles, the remainder are HNGs with varying diameters and wall thicknesses. (Reprinted with permission from ref. 74. Copyright 2006, American Chemical Society.)

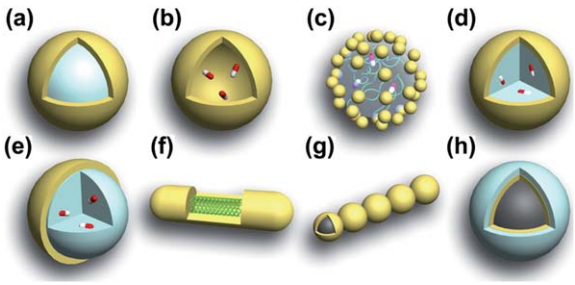

Fig. 13 Various forms of therapeutic gold nanoshell structures. (a) Silica/polymer–gold core–shell particle. (b) Gold nanoshell particle without the core. (c) Gold cluster-coated liposome particle. (d) Polymer–gold core–shell particle. (e) Janus-type core–shell particle. (f) Gold coated-carbon nanotube. (g) Gold coated-metal oxide nanoparticle chain. (h) Multi-layered gold nanoshell particle.

can be precisely tuned by controlling the shell thickness (Fig. 12). The most common gold nanoshell structure is a thin layer of gold shell formed on a silica or polymeric nanocore (Fig. 13a). The core–shell structure was made in the exploitation of its plasmon resonance for applications such as thermal ablation, tumor imaging and thermal-triggered drug delivery.[46,76,77] The application of gold nanoshells for photothermal therapy of cancer was first established by Halas and colleagues in 2003.[76] In their work, gold nanoshells made by using silica nanoparticle templates were used to target breast carcinoma cells. On NIR irradiation, the temperature in the vicinity of the target increased to a range between 40 to 50 °C and subsequently destroyed the carcinoma. In addition to silica/gold core–shell structures, gold hollow nanoparticles can be regarded as another type of nanoshell structures (Fig. 13b). The hollow structures can provide high capacity of drug loading and generate strong photothermal effects because of their strong surface plasmon absorption band centered in the NIR region.

Much work has recently gone into the development of more complex core–shell nanostructures for specific therapeutic applications. Romanowski and co-workers[47] have reported a new method for light-triggered content release from liposomes coated with a shell-shaped array of discrete gold clusters. In response to irradiation of a NIR light, the metastable liposomes can undergo a phase-transition as the energy absorbed by the gold clusters is converted into heat. This enables light-controlled release of the drug content entrapped by the liposomes (Fig. 13c).

Yang *et al.*[78] have fabricated a nanotherapeutic system consisting of a doxorubicin-loaded biopolymer matrix and a gold overlayer. This system has a dual function as the therapeutic agent carrier and heat-generating probe (Fig. 13d). The combination of chemotherapy and photothermal treatment may lead to substantial improvement of therapeutic effectiveness. As a parallel development, Yoo and co-workers[79] have reported the facile delivery of doxorubicin *via* a Janus-type half-shell structure (Fig. 13e). A multimodal therapeutic system based on gold-plated carbon nanotubes has also been reported for targeting lymphatic vessels in mice (Fig. 13f).[80] To enhance the efficiency of drug delivery, Yu and co-workers have fabricated hydrophilic magnetic yolk/shell nanoparticles.[81] These nanoparticles have the feature of a cobalt core and a porous gold nanoshell. Under an external magnetic field, the nanoparticles form an interesting "peas in a pot" structure that can be used as a nonviral vector for gene delivery and transfection (Fig. 13g). Multifunctional magnetic gold nanoshells (Fig. 13h) have also been demonstrated by the groups of Hyeon, Li, Haam, Diaz and Chen.[78,82–86] More recently, Gao and co-workers[87] have developed an interesting type of magnetic gold nanoshells composed of an iron oxide core, a dielectric polymer middle layer and a gold shell. These multifunctional nanoparticles exhibited multimodal imaging capabilities highly sensitive to optical, magnetic and thermal stimulation.

The photothermal conversion efficiency between gold nanorods and nanoshells has been a matter of much debate. Yeh and co-workers[88] demonstrated that the conversion efficiency of gold nanoshells is greater than that of gold nanorods, as quantified by measuring the number of the particles required to kill malignant cells under identical reaction conditions. El-Sayed and co-workers,[89] however, concluded that in terms of absorption and extinction, nanorods are an order of magnitude more effective than nanoshells containing a similar volume of gold. To compare gold nanorods and nanoshells in photothermal conversion efficiency on the basis of overall particle volume, Maltzahn *et al.*[90] have carried out both computational and experimental studies. They observed that nanorods exhibited an extinction coefficient three times higher than nanoshells. The low absorption efficiency of nanoshells at a given wavelength can be, in part, attributed to considerable electron scattering effects that result in the problems of attenuation and broadening of the plasmon resonances. On a practical level, unlike nanorods with surface plasmon resonance readily tunable into the infrared by increasing their aspect ratios, such tuning in nanoshells may present a substantial challenge as the shell thickness has to be reduced to problematic dimensions (~5 nm).

3.4 Nanocages

Gold nanocages are a novel class of therapeutic nanomaterials with hollow interiors and porous walls.[91–93] Developed by Xia and co-workers, these nanocages have cubic shape with pores formed in the clipped corners of the cubes. The nanocages have strong absorption in the NIR spectral region, which is useful for developing NIR-mediated drug-release systems. For example, Xia and co-workers[91] have recently demonstrated the application of such a nanocage system for controlled drug release (Fig. 14). Gold nanocages were prepared by the galvanic replacement reaction between silver nanocube precursors and $HAuCl_4$ (or $HAuCl_2$) in an aqueous solution. The nanocages were covered with a monolayer of smart polymers composed of poly(*N*-isopropylacrylamide) and its derivatives. The polymers serve as molecular switches that change conformation in response to small variations in temperature. On exposure to a NIR laser with a wavelength matching the absorption peak of the gold nanocage, the light was absorbed and converted into heat through the photothermal effect. The heat subsequently dissipated into the polymers and allowed the nanocages to switch to the on state. The drug release can be switched off if the polymers changes back to their original, extended conformation by turning off the external laser. Importantly, a precise control over the drug dosage can be achieved through fine tuning of the irradiation time or laser flux density on the nanocages.

4. Magnetic nanoparticles

Magnetic nanoparticles are an important class of nanomaterials that consist of typical magnetic elements such as iron, nickel, cobalt, manganese, chromium and gadolinium, as well as their chemical compounds. Recently, these materials have attracted significant interest in biomedical research because they provide advanced therapeutic capabilities with dual-mode manipulation controlled either by using a magnetic field or through surface ligand engineering.

From a therapeutic point of view, the suitability of magnetic nanomaterials is largely determined by three factors: toxicity, magnetic performance and biocompatibility.[94,95] According to the present clinical standards iron and manganese elements are considered nontoxic, whereas cobalt and chromium are highly toxic to biological systems. Therefore, magnetic nanomaterials based on the nontoxic elements, especially iron and its oxidized form, have been widely investigated for therapeutic applications.[96–100]

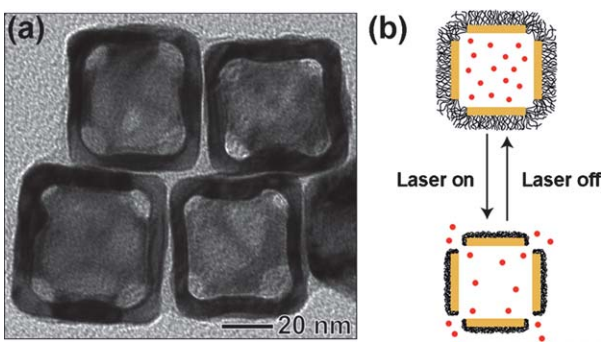

Fig. 14 (a) TEM image of polymer-coated Au nanocages prepared by Xia and co-workers. The photo shows a high-magnification TEM image of a gold nanocage. (b) Schematic representation of laser light-responsive conformation change of the polymer that leads to the release of the drug molecules encapsulated in the nanocage. (Reprinted with permission from ref. 91. Copyright 2009, Nature Publishing Group.)

In addition to iron-based nanoparticles, various types of magnetic nanomaterials based on lanthanide-doped nanoparticles have been systematically explored. For example, Gd^{3+}-doped nanoparticles have been used in thermal therapy for treatment of cancer due to their high specific power adsorption rate.[101] Other lanthanide dopant ions (such as Sm^{3+}, Eu^{3+}) have also been utilized to fine tune the magnetic property of the nanoparticles.[102] Reliable magnetic performance is another significant requirement to a magnetic nanosystem, but the performance of some metal and alloy nanomaterials (*e.g.*, Fe and FeCo nanoparticles) with high magnetization is often compromised by their ease of oxidation and corrosion. However, these limitations can be overcome through a proper surface coating of the nanomaterials with biocompatible substances such as poly (ethylene glycol) (PEG), dextran, carbon or inert metals.

Sun and colleagues[119] have recently developed iron oxide nanoparticles with four types of PEG polymers covalently tethered to the particle surface *via* the chelating *o*-catechol moiety of dopamine. These nanoparticles exhibited excellent aqueous dispersity. Another notable demonstration was reported by Seo *et al.*[120] who developed a chemical vapour deposition technique to manufacture FeCo nanocrystals coated with a thin graphitic shell. Because of surface coverage of the graphitic shell, these nanoparticles exhibited good biocompatibility and no obvious toxicity issues under both *in vitro* and *in vivo* investigations.

Magnetic nanoparticles covered with a biocompatible coating and functional ligands may serve as powerful platforms for therapeutic use in advanced magnetic resonance imaging (MRI), drug delivery, gene regulation, hyperthermia cancer therapy and cell tracking (Table 2).[121–125] In one example, Sun and co-workers[126] have synthesized dumbbell-like Au-Fe_3O_4 nanoparticles surface-modified with platin molecules and Her2-specific antibody (Fig. 15). After incubation of the platin–nanoparticle conjugates with Sk-Br3 and MCF-7 cells, light microscopy experiments showed that the conjugates bind to Sk-Br3 cells with greater affinity than the MCF-7 cell control. The specific targeting thus enables efficient delivery of platinum-based anticancer drugs to malignant cells. Sun and co-workers[113] have also developed biocompatible FePt nanoparticles that are stable under neutral pH conditions in a tumor cell, but capable of releasing Fe content under a low pH (4.8) environment. The hydrogen peroxide generated by mitochondrial respiration can be converted by the Fe catalyst into highly reactive oxygen species (ROS) such as hydroxyl radicals. This could lead to membrane lipid oxidation and cell death. Coupled with cancer-targeting antibody or peptide (*e.g.* luteinizing hormone-releasing hormone peptide), the FePt nanoparticles should provide promising applications to target-specific therapeutics (Fig. 16).

5. Luminescent nanoparticles

Conventional fluorescent probes, such as dye molecules and metal-chelating complexes, are frequently used biomarkers for

Table 2 Selected magnetic nanomaterials in therapy[a]

Composition	Size	Therapeutic mechanism	Therapeutic targets	Experimental conditions	Ref
Polymer-Fe_3O_4 Janus particles	Fe_3O_4 (~5 nm)	Magnetolytic therapy	Prostate tumor LNCaP cells	*In vitro*	103
Dextran-coated iron oxide particles	~30 nm	MMOCT and 3D MRI	Inbred Wistar–Furth female rats	*In vivo* and *ex vivo*	104
Polylactide-based Fe_3O_4 particles	~263 nm	Drug delivery	Rat carotid stenting	*In vivo*	105
Fe_3O_4-silica hybrid particles	Silica (~70 nm); magnetite (~8.5 nm)	MRI and drug delivery	B16–F10 cells *in vitro* and mouse tumor *in vivo*	*In vitro* and *in vivo*	106
Sugar-coated Fe_3O_4 particles	~6 nm	MRI and cell adhesion suppression	B16–F10, B16–F1, MCF-7, TA3-HA and TA3-ST cells	*In vitro*	107
PEG-coated iron oxide particles	~13.5 nm	MRI	Mouse xenograft tumor and tissue	*In vivo*	108
BSA-based $CoFe_2O_4$ particles	$CoFe_2O_4$ (~6.7 nm)	MRI and hyperthermic therapy	HeLa cancer cells	*In vivo* and *in vitro*	109
Hap and NBM coated Fe_3O_4 particles	~300 nm	Magnetofection and cell therapy	Mesenchymal stem cells	*In vitro*	110
Au-coated Fe/Ni permalloy discs	Disc thickness (~60 nm)	Mechanical force intervention	N10 cells	*In vitro*	111
PAH/PAA-coated Fe_3O_4 particles	Core (15–20 nm); shell (8–70 nm)	Platinum anti-cancer drug delivery	Prostate cancer PC3 cells	*In vitro*	112
Phospholipid-coated FePt particles	~9 nm	Reactive oxygen-mediated cell damage	A2780 cells	*In vitro*	113
Lipid-coated Fe_3O_4 particles	~40, 71, 146 nm	Gene delivery and silence	MKN-74- and NUGC-4-innoculated mice	*In vivo* and *in vitro*	114
Lentiviral vector-coupled particles	—	Gene transfer	Mouse carotid artery	*In vivo* and *ex vivo*	115
PEG/dopamine-coated Fe_3O_4 particles	~12 nm	Drug delivery and release	HeLa cells	*In vitro*	116
Silica-coated Fe_3O_4 particles	Fe_3O_4 core (~15 nm); shell (~40 nm)	MRI and drug delivery	Mouse tumor	*In vivo*	117
MFL AS: commercial magnetic particles	~15 nm	Hyperthermic therapy	Prostate cancer	*In vivo*	118

[a] MMOCT: Magnetomotive optical coherence tomography; MRI: magnetic resonance imaging; BSA: bovine serum albumin; Hap: hydroxyapatite; NBM: natural bone mineral; PAA: poly(acrylic acid); PAH: poly(allylamine hydrochloride).

biochemical and cellular assays as they enable researchers to encode chemical information with almost unsurpassed sensitivity. These molecular probes also have tremendous promise in accelerating the drug evaluation process. Most common molecular probes, however, have significant drawbacks for therapeutic and diagnostic imaging applications. These drawbacks include low photostability, broad emission spectra and the

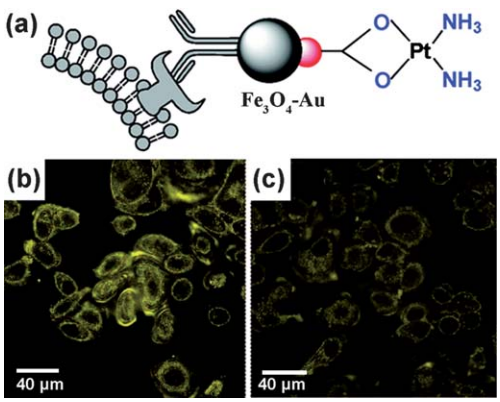

Fig. 15 (a) Schematic diagram of the dumbbell-like Au-Fe_3O_4 NPs coupled with herceptin and a platin complex for target-specific platin delivery. Reflection images of (b) Sk-Br3 and (c) MCF-7 cells after incubation with the same concentration of platin–Au–Fe_3O_4–herceptin NPs. (Reprinted with permission from ref. 126. Copyright 2009, American Chemical Society.)

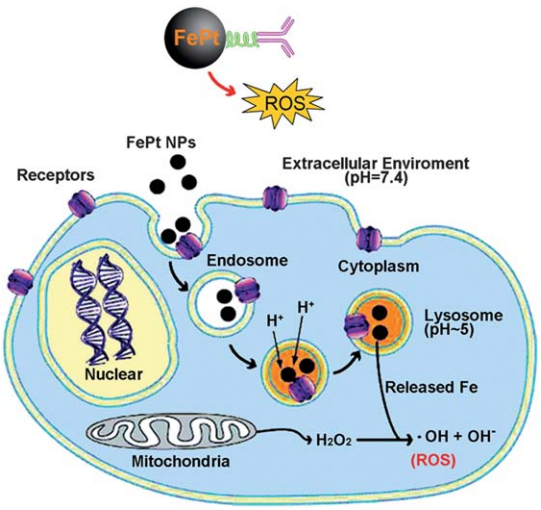

Fig. 16 Schematic diagram showing the release of Fe content from FePt nanoparticles in a malignant cell and tumor inhibition by ROS generated from the Fe-catalyzed reaction. (Reprinted with permission from ref. 113. Copyright 2009, American Chemical Society.)

need of different excitation wavelengths for multiplexed cell labeling and molecular tracking.[127] Recent reports have demonstrated that semiconductor quantum dot and upconversion nanoparticle labels can overcome the limitations associated with molecular probes and positively impact the field of therapeutics.

5.1 Semiconductor quantum dots

Semiconductor quantum dots are nanometer-sized particles of group II–VI or III–V atoms from the periodic table of elements. These nanoparticles are smaller than the exciton Bohr radius (typically 1–10 nm in size).[129,130] As a result, quantum dots exhibit quantum confinement effects, resulting in optical properties that are significantly different than the corresponding bulk material. By varying particle size and chemical composition, the fluorescence emission can be fine-tuned from blue up through the infrared.[131–136] For example, cadmium sulfide (CdS) and zinc selenide (ZnSe) dots can be prepared to emit blue to near-UV light, while cadmium selenide (CdSe) can emit light across the entire visible spectrum.[137] In 1998, Alivisatos[138] and Nie[27] independently demonstrated that quantum dots can be made water soluble and tagged to biological molecules. Since then, quantum dots have attracted widespread interest in biology and medicine for tagging and tracking biological species. Although there are concerns over cytotoxic effects with the quantum dots in 2D cultures, recent studies by Kotov and colleagues[128] have shown that the cytotoxic effects are significantly minimized in the 3D spheroid cell cultures (Fig. 17).

Tumor targeting and imaging. In contrast to commercial organic fluorophores, quantum dots exhibit slightly low quantum yields of 40–50%. This is compensated by the high molar extinction coefficients of such particles at 10^5–10^6 M^{-1} cm^{-1}, which is 10–100 times larger than those for typical organic fluorophores.[138] The quantum dots are also highly resistant to photobleaching, which enables visualization of biological samples over extended periods of time. Studies have shown that CdSe dots can be made to seep into cancerous tumors in the body. When exposed to light, the particles emit visible light for visualization of sick cells *in vivo*.[139–146] An elegant example was demonstrated by Nie and co-workers[147] for *in vivo* tumor targeting and imaging by single chain epidermal growth factor receptor (EGFR) antibody conjugated quantum dots (Fig. 18). After systemic delivery, efficient internalization of the nanoparticles into pancreatic cancer cells was clearly observed.

Photodynamic therapy. Despite their significant potential benefits to drug delivery and imaging, quantum dots were not utilized for direct cancer therapy until 2003 in the demonstration by Samia *et al.*[148] They showed that quantum dots can exhibit cytotoxic effects, mediated by UV irradiation, as a means of killing malignant cells. Quantum dots in their "dark states" can transfer energy through a mechanism termed as triplet energy transfer (TET) to molecular oxygen and induce the generation of reactive oxygen species (Fig. 19a). Alternatively, quantum dots can act as cofactors to promote the effect of conventional photosensitizing agents used in photodynamic therapy (PDT) *via* Förster resonance energy transfer (FRET) (Fig. 19b). Quantum dots offer several advantages over conventional molecular photosensitizers. They have large absorption cross-section, persistent generation of singlet oxygen ($^1O_2$) under prolonged and repetitive irradiation, and the possibility to generate $^1O_2$ under excitation in the NIR spectral region where biological tissues are optically transparent. Relative to conventional photosensitizers with $^1O_2$ yields ranging from 40 to 60%, quantum dots typically have a low $^1O_2$ quantum yield (~5%),

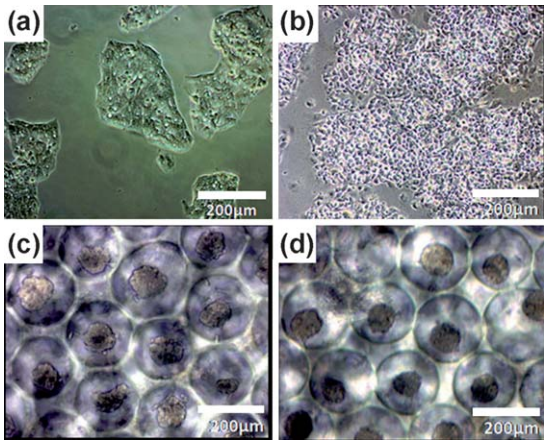

Fig. 17 Comparison of 2D and 3D cultures of HepG2 cells after incubation with CdTe nanoparticles for 12 h. (a) and (c) optical images of normal 2D and 3D spheroid cultures, respectively. (b) and (d) The corresponding optical images of 2D and 3D cell cultures after incubation with the particles, respectively. The 2D culture showed a dramatically different morphology, while no significant change was observed for the 3D culture. (Reprinted with permission from ref. 128. Copyright 2009, Wiley-VCH Verlag GmbH & Co. KGaA.)

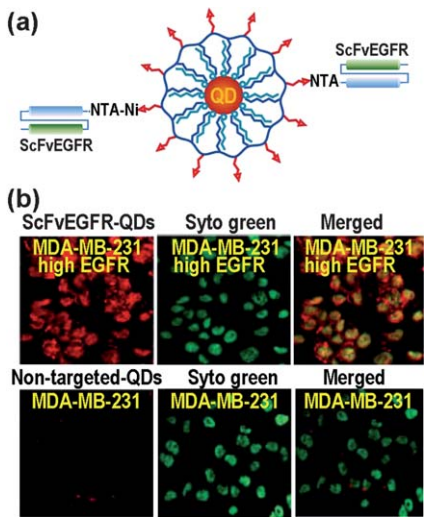

Fig. 18 Specificity examination of ScFvEGFR-conjugated quantum dots for targeting tumor cells. (a) Schematics showing polymer coating of quantum dots and bioconjugation with Ni-NTA. (b) Comparative optical images of tumor cells incubated with or without the particles. Selective internalization of the particles in tumor cells was determined using cancer cell lines expressing a high (MDA-MB-231) level of EGFR. Strong red fluorescent signal was detected inside MDA-MB-231 cells incubated with the particles, but not with non-targeted particles. (Micrographs are reprinted with permission from ref. 153. Copyright 2009, Wiley-VCH Verlag GmbH & Co. KGaA.)

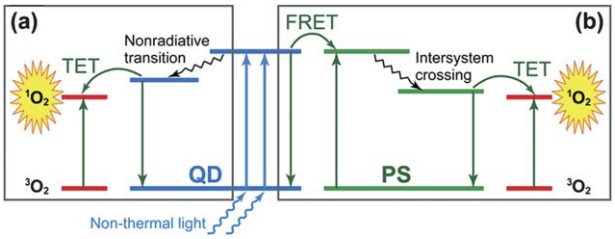

Fig. 19 Two possible pathways of quantum dot-induced generation of singlet oxygen. (a) The quantum dot (QD) directly interacts with molecular oxygen through triplet energy transfer (TET) to generate singlet oxygen. QD with energy of triplet state larger than 0.97 eV (the energy of singlet oxygen) is required to activate triplet oxygen. (b) QD acts as a cofactor to promote the effect of a conventional photosensitizer (PS) through FRET.

possibly due to carrier trapping by surface defect sites and nonradiative carrier recombinations.[148–150] Nevertheless, the effectiveness of quantum dots to provoke apoptosis in tumor cells can be increased by prolonged photoactivation.[151,152] It may also be possible to improve the $^1O_2$ generation by reducing the defect sites through additional surface passivation.

The concept of using quantum dot–photosensitizer hybrid systems for PDT was first envisaged by Samia *et al.*,[148] who demonstrated a non-covalent mixture composed of 5-nm CdSe quantum dots and a silicon phthalocyanine (Pc4) photosensitizer. Encouragingly, a FRET efficiency of 77% was obtained in this system. As quantum dots can be excited by any wavelength spanning from the visible to NIR spectral regions, construction of quantum dot–photosensitizer systems through a variety of chromophores or acceptors is possible by selecting appropriate quantum dot donors.[150] Although non-covalent mixing of quantum dots and photosensitizers is applicable to the FRET process, covalent conjugation of the photosensitizers with quantum dots is desirable. Such preference is relevant for efficient $^1O_2$ production as the transfer rate varies inversely with the sixth power of the donor–acceptor separation. A recent review by Medintz and Mattoussi[154] provides excellent and extensive coverage of various donor–acceptor systems.

Quantum dots are enormously exciting new materials for PDT, but they still have significant problems with cytotoxicity, biocompatibility and complex photophysics such as blinking. The cytotoxicity problem of quantum dots can be somewhat ameliorated by coating with silica and polymer layers[155] or through use of heavy metal-free quantum dots.[156] The efficacy of quantum dot-based systems for *in vivo* PDT studies is an additional major challenge to overcome. Therefore, the fabrication of quantum dot–photosensitizer systems that enable improved therapeutic effects in living organisms would be highly desirable.

5.2 Lanthanide-doped upconversion nanoparticles

Lanthanide-doped nanoparticles typically comprise an insulating host material and lanthanide dopant ions embedded in the host lattice.[22,157–162] The luminescence of lanthanide-doped nanomaterials primarily originates from intra-configurational $4f^n$ electron transitions within the localized dopant ions. In stark contrast to quantum dots, quantum confinement effects are typically not expected in lanthanide-doped nanomaterials due to small Bohr radius of the exciton in the host, as well as weak interaction between the $4f^n$ electrons of the dopant ions and the host material. As a result, the luminescence properties of lanthanide-doped nanomaterials closely resemble those of the bulk counterparts. The emission profiles of lanthanide-doped nanomaterials are usually manipulated by varying dopant compositions and concentrations in the host lattice.[15,163–173]

As lanthanide-doped nanoparticles generally contain nontoxic elements and offer extremely stable luminescence against photobleaching and optical blinking, they have been suggested as alternatives to quantum dots as luminescent probes for biomedical studies. For example, Alexandrou and co-workers[174] have demonstrated specific targeting and imaging of Na^+ channels in live cardiac myocytes by using guanidinium-functionalized YVO_4:Eu nanoparticles. They showed that the nanoparticles are individually detectable in the heart muscle cells without emission intermittency, thus providing potential use for long-term single molecule tracking. However, little progress has been made on biomedical applications of these nanoparticles in recent years. This is mainly attributed to the need of deep ultraviolet excitation which is harmful to biological systems. Therefore, current research on lanthanide-doped nanoparticles is primarily focused on those capable of converting NIR excitation into the visible range in a process known as photon upconversion (UC).[22,175–178]

Photon UC processes are unique nonlinear optical phenomena that convert two or more low-energy pump photons into a higher-energy output photon through sequential photon absorption. Such anti-Stokes processes, recognized in the mid-1960s, have attracted significant research interest for their applications in optical devices such as infrared quantum counter detectors and compact solid state lasers. The current focus on UC-based bioimaging and therapy owes to the foundations of nanoscience laid down with the discovery of synthetic methods for preparing ultrasmall UC nanoparticles in late 1990s.

Advances in synthetic methods. As discussed earlier, nanoparticles for biomedical application should have a small particle size and good dispersity for integration with biological molecules and macromolecules. To this end, a variety of techniques, including coprecipitation, thermal decomposition, hydrothermal synthesis, sol–gel processing, combustion and flame synthesis, have been developed for the synthesis of UC nanoparticles featuring high crystallinity, dispersity, and well-defined crystal phase and size (Fig. 20).[12,22,171,179–181,184–204] As an outstanding demonstration, Murray and co-workers[179] have shown that monodisperse $NaYF_4$ nanoparticles with controlled shapes can be prepared by using the thermal decomposition method. They showed that under appropriate conditions the as-synthesized UC nanoparticles can be assembled into large-area superlattices (Fig. 20a and b). However, one of the constraints associated with these techniques is the need of simultaneous control over a number of reaction conditions, such as high reaction temperature and prolonged reaction time. Recently, we have developed a Gd^{3+}-doping method that allows the facile formation of UC nanoparticles with small feature size and controlled crystal phase (Fig. 20e).[182] The lanthanide-doping approach to phase transformation was also confirmed by several other groups.[205–207] More recently, Wang and co-workers[183,208] have extended the

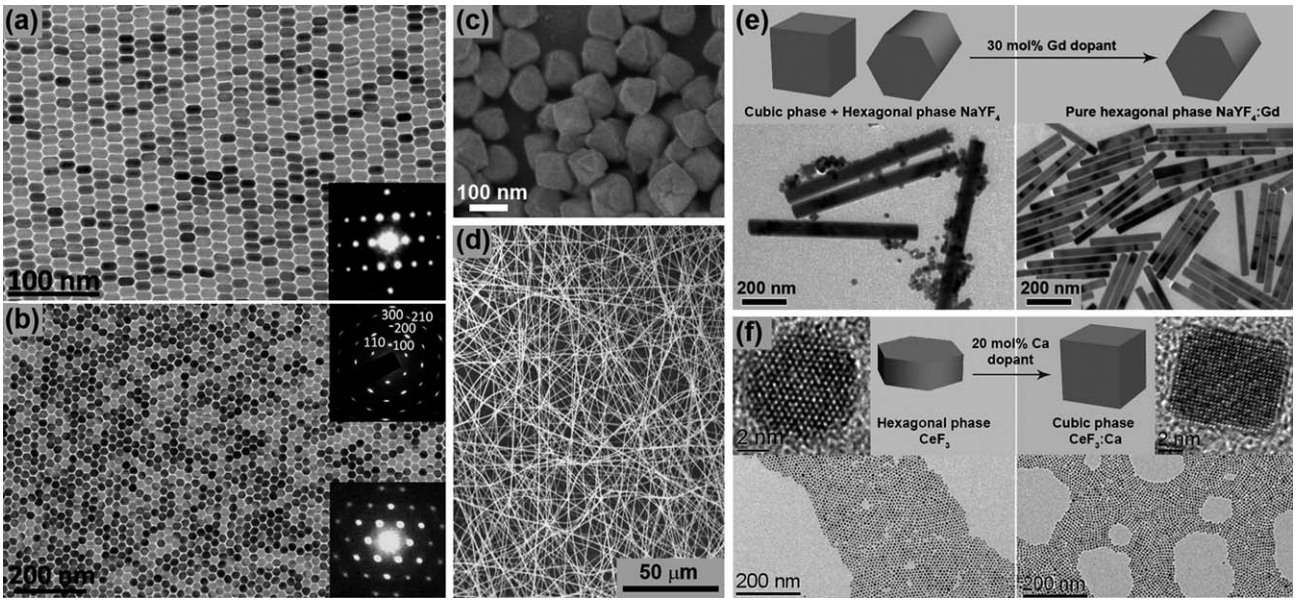

Fig. 20 (a, b) Transmission electron microscopy (TEM) images by Murray and co-workers showing monolayer superlattices of monodisperse $NaYF_4$ nanorods that are oriented parallel and vertically to the substrate, respectively. Inset (a) shows the corresponding small-angle electron diffraction (SAED) pattern. The upper right and lower right insets of (b) are the corresponding wide-angle electron diffraction patterns (SAWED) and SAED patterns, respectively. (c) Scanning electron microscopy (SEM) image of lanthanide-doped YF_3 nanooctahedra fabricated by Qin and co-workers. (d) SEM image of the $NaYF_4$-polyvinylpyrrolidone composite fibers fabricated by Song and co-workers. (e) TEM images showing simultaneous phase and size control of $NaYF_4$ nanoparticles through Gd^{3+} doping by Liu and co-workers. (f) TEM images showing simultaneous phase and morphology control of CeF_3 nanoparticles through Ca^{2+} doping by Wang and co-workers. (Reprinted with permission from (a, b) ref. 179, (c) ref. 180, (d) ref. 181, (e) ref. 182 and (f) ref. 183. Copyright 2010, 2009, 2008, 2010, 2011, respectively, National Academy of Sciences, USA, Elsevier B.V., American Chemical Society, Nature Publishing Group and Royal Society of Chemistry.)

doping strategy for the controlled synthesis of MF_2 (M = Ca, Sr and Ba) and LnF_3 (Ln = La, Ce and Pr) nanoparticles (Fig. 20f).

Emission enhancement. The emission profile of common UC nanoparticles is influenced by the particle size and solvents, restricting their capacity to visualize molecular or cellar activities under varying physiological conditions. To overcome particle size-induced loss in UC emission intensity, core–shell nanoparticles that comprise a particle core and an epitaxial shell coating have been prepared by the research groups of Yan, Capobianco, Chow, van Veggel, Patra, Chen and Hasse.[209–216] In the core–shell design, lanthanide dopants are confined within the core particle and protected from surface quenching by solvent and ligand molecules. For example, we have recently observed a luminescence enhancement of nearly 500 times for $NaGdF_4$:Yb/Tm nanoparticles (~10 nm) coated with 2.5-nm thick $NaGdF_4$ shells.[217]

Alternatively, the emission intensity of UC nanoparticles can be enhanced by coupling the particles to metallic surfaces.[218–221] One study by Yan and co-workers[218] determined that enhancement factors of 2.3 and 3.7 are obtained for green and red emission of $NaYF_4$:Yb/Er nanoparticles through use of silver nanowires (Fig. 21a). Their controls showed that the emission enhancement is highly dependent on the size of metallic nanowires. In a parallel development, Schietinger and co-workers[219] have reported increased UC emission for a single $NaYF_4$:Yb/Er nanoparticle in the vicinity of gold nanospheres. Changes in excitation and emission processes were correlated with plasmonic effects of the metal particles (Fig. 21b). Plasmonic modulation of UC emission in UC nanoparticles has also been demonstrated by Duan and co-workers (Fig. 21c, d).[221] However, the challenge remains for preparing such hybrid nanoparticles on large scale by using a convenient synthetic method.

Bioconjugation and imaging. The bioconjugation of UC nanoparticles as contrast agents for biomedical diagnosis and imaging has been extensively investigated by a number of independent research groups. Several important conclusions can be drawn from these studies. First, it is clear that the UC nanoparticles can offer high signal-to-noise ratios and thus high sensitivity assays.[12,224–228] Second, these nanoparticles do not suffer from photo-blinking (intermittent emission), enabling reliable single-molecule tracking.[229,230] In addition, we could directly use UC nanoparticles in high contrast *in vivo* imaging for probing dynamic events in living cells and transparent organism studies.[212,231–239] Imaging of organs and organ function *in vivo* has mainly been advanced by magnetic resonance imaging (MRI), positron emission tomography (PET) and ultrasound techniques. These technologies provide molecular selectivity, but lack substantial spatial resolution. Kobayashi *et al.*[222] reported use of $NaYF_4$ nanocrystals for imaging lymphatic channels and nodes of mouse with remarkable spatial resolution (Fig. 22a). They demonstrated that the UC nanoparticles are sufficiently bright to enable *in situ* imaging during surgery. In a more recent development, Liu and co-workers[223] showed that multicolored UC nanoparticles can be used for multiplexed *in vivo* lymph node mapping (Fig. 22b). In contrast to the detectability with quantum dots, a greater than 10-fold improvement was obtained

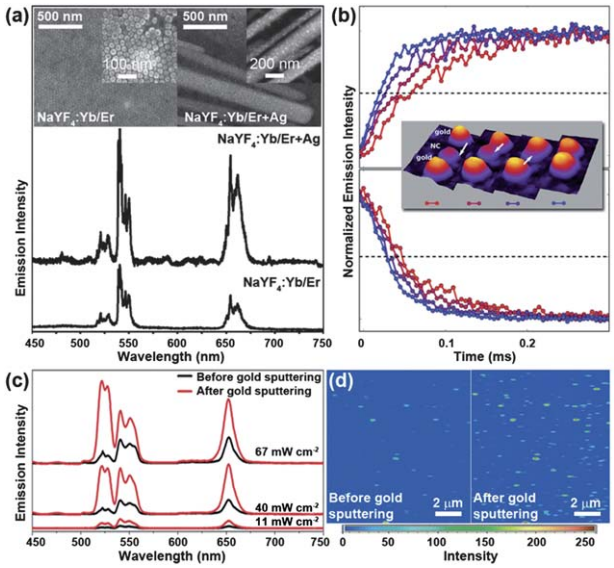

Fig. 21 (a) UC emission enhancement through use of silver nanowires by Yan and co-workers. (b) Tuning emission by Schietinger and co-workers of a single UC nanoparticle in the vicinity of gold nanoparticles through controlling the inter-particle distance. (c) Emission enhancement through gold sputtering by Duan and co-workers. The emission spectra of $NaYF_4$:Yb/Er nanoparticles were obtained upon 980 nm excitation of the particles with or without the sputtered gold at varied power densities. (d) Corresponding confocal luminescence images of the particles with or without sputtered gold. The metal-induced enhancement in UC emission is evident. (Reprinted with permission from (a) ref. 218, (b) ref. 219 and (c, d) ref. 221. Copyright 2009, 2010, 2011, respectively, Royal Society of Chemistry and American Chemical Society.)

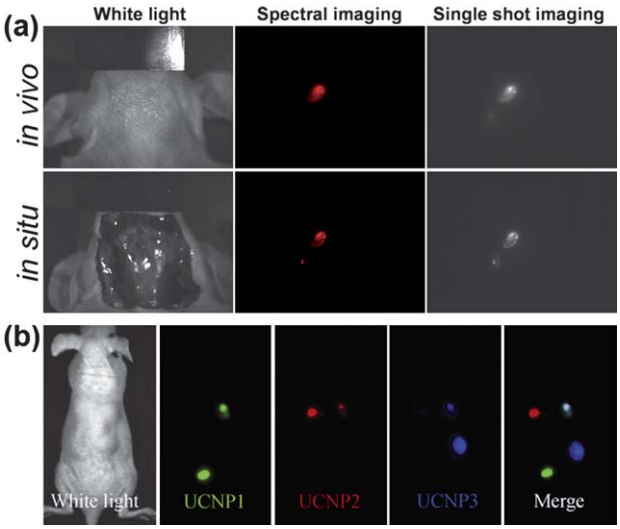

Fig. 22 (a) Spectral and single-shot lymphatic imaging with NIR-to-NIR UC nanoparticles. (b) Multiplexed imaging of a nude mouse with multicolor UC nanoparticles. (Reprinted with permission from (a) ref. 222 and (b) ref. 223. Copyright 2009, 2010, Royal Society of Chemistry and Tsinghua University Press and Springer.)

by using UC nanoparticles. Combination of different therapeutic modalities is also possible for multimodal imaging with nanometer spatial resolution and molecular selectivity. To enable correlation of different types of imaging, a primary approach is

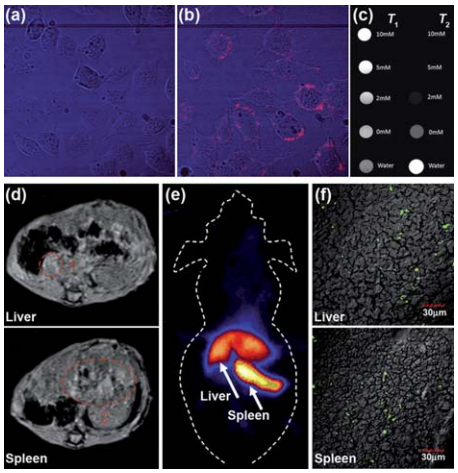

Fig. 23 (a–c) Luminescence and MR imaging using $NaYF_4$:Yb/Er/Gd nanoparticles by Prasad and co-workers. (a,b) Confocal images of Panc 1 cells treated with non-bioconjugated and anti-claudin 4-conjugated particles, respectively. (c) T_1- and T_2-weighted MR images of particles doped with varying Gd^{3+} content. (d–f) Multimodal imaging using ^{18}F-labeled $NaYF_4$:Gd/Yb/Er nanoparticles by Li and co-workers. (d) Cross-sectional MR images of the mouse liver (region 1) and spleen (region 2) taken after injection of the particles for 15 min. (e) Whole-body PET image acquired at 15 min after intravenous injection of the particles. (f) Overlaid images of liver and spleen sections stained with the particles. (Reprinted with permission from (a–c) ref. 240 and (d–f) ref. 242. Copyright 2009, 2011, respectively, Wiley-VCH Verlag GmbH & Co. KGaA and Elsevier B.V.)

to construct particle probes that can be monitored by multiple modalities at once.[240–243] For example, Prasad and co-workers[240] have doped lanthanide ions with upconverting (Yb/Er) and magnetic (Gd) properties in $NaYF_4$ nanoparticles for dual-mode optical imaging and MRI (Fig. 23a–c). More recently, Li and co-workers[242] developed a new generation of ^{18}F-labeled $NaYF_4$: Gd/Yb/Er nanoparticles that possess radioactivity, magnetism and UC luminescence properties (Fig. 23d–f). They also demonstrated use of the particles for *in vivo* PET, MRI and *ex vivo* UC luminescence imaging. This study is important as it enhances the sophistication by which physiological processes can be examined, from biomolecular events occurring at the cellular level to the coordinated whole-body functions.

Drug delivery. UC nanoparticles have also been used to store and deliver drugs. The synthesis of porous particles is a straightforward solution to developing drug carriers. However, rational control of the pore size and density without affecting UC emission of the particles is practically inaccessible. An attractive alternative is to coat the particles with a porous silica layer which is permeable to drug molecules. In one example, Lin and co-workers[244] developed a bifunctional core–shell nanocomposite comprising a Gd_2O_3:Er core and a mesoporous silica shell (Fig. 24a–d). As a proof-of-concept experiment, they showed that ibuprofen molecules, adsorbed onto the surface of mesoporous silica in hexane solution, can be released to media mimicking body fluids by a diffusion-controlled mechanism. By using a similar method, Zhang and co-workers[245] have prepared core–shell LaF_3:Yb/Er nanoparticles (Fig. 24e–i). Parallel advances have also been made by Branda and co-workers[246,247]

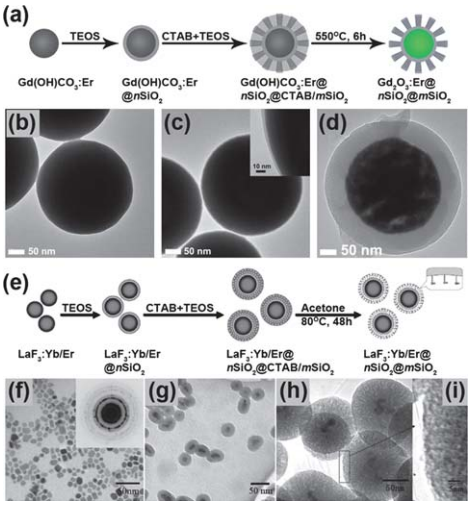

Fig. 24 (a) Synthetic scheme developed by Lin *et al.* for core–shell Gd_2O_3:Er@nSiO$_2$@mSiO$_2$ nanoparticles. (b–d) Corresponding TEM images of the Gd_2O_3 particles obtained at different stages. (e) Synthetic scheme developed by Zhang *et al.* for core–shell LaF_3:Yb/Er@nSiO$_2$@mSiO$_2$ nanoparticles. (f–i) Corresponding TEM images of the LaF_3 particles obtained at different stages. (Reprinted with permission from (a–d) ref. 244 and (e–i) ref. 245. Copyright 2011, 2010, respectively, Royal Society of Chemistry and Wiley-VCH Verlag GmbH & Co. KGaA.)

on the controlled release of cage compounds through use of UC nanoparticles, providing an effective route to spatial and temporal control of drug delivery.

Temperature monitoring. The green emission of Er^{3+} ion consists of two distinct bands at 525 and 545 nm corresponding to electronic transitions from $^2H_{11/2}$ and $^4S_{3/2}$ to the ground state, respectively. Due to the close proximity ($\Delta E = 700$ cm^{-1}) of the two states, a thermal equilibrium occurs governed by the Boltzmann factor.[248] As a result, the relative intensity ratio of 525 to 545 nm emissions depends strongly on temperature and provides an accurate probe of operating temperature of biological systems with submicrometric resolution.[248] For example, Aigouy and co-workers[249] have modified an atomic force microscope scanning cantilever with PbF_2:Yb/Er nanoparticles and used it for measuring the heating of electrically excited micro- or nanowires (Fig. 25a). They achieved a relative sensitivity of 1.1% K^{-1} at ~310 K. Another intriguing recent development was reported by Capobianco and co-workers,[250] who showed that $NaYF_4$:Yb/Er nanoparticles internalized by HeLa cancer cells can be used to accurately measure the internal temperature of a single living cell (Fig. 25b).

Photodynamic therapy. Of particular note is the impact of UC nanoparticles are likely to have on the effect of PDT. Our recent review,[12] as well as those of several other research groups,[251–253] have highlighted that UC nanoparticles, when functionalized with a selected number of photosensitizers, provide efficient therapy in deep biological tissues. UC nanoparticles are advantageous over alternative systems for PDT applications in that these particles can activate photosensitizers on NIR laser excitation (Fig. 26). Moreover, the energy transfer from the particle to photosensitizer is dominated by lanthanide resonance energy

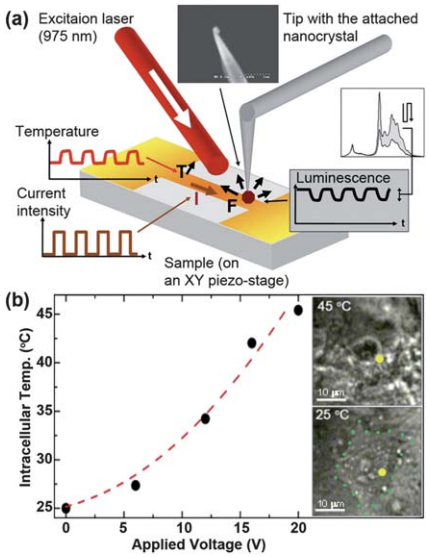

Fig. 25 (a) Schematic of UC nanoparticle-based thermal measurement developed by Aigouy and co-workers through use of an atomic force microscope (AFM) and an electrically excited micro or nanowire. The device is powered by a square electrical current (brown curve) that induces a periodic Joule heating (red curve) and a luminescence quenching of the particle (black curve). The inset shows the UC particle attachment to the AFM cantilever. (b) UC nanoparticle-based temperature monitoring in single cells developed by Capobianco and co-workers. The temperature was determined by measuring the Er^{3+} luminescence as a function of the applied heating voltage. The inset shows optical transmission images of an individual HeLa cell recorded at two different temperatures. Cell death was observed at 45 °C. (Reprinted with permission from (a) ref. 249 and (b) ref. 250. Copyright 2009, 2010, respectively, American Institute of Physics and American Chemical Society.)

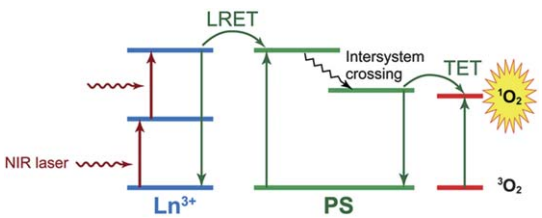

Fig. 26 Proposed mechanism of UC nanoparticle-induced generation of singlet oxygen. The incident NIR photons are absorbed by the Ln^{3+}-doped UC nanoparticles, which subsequently activate a conventional photosensitizer (PS) *via* a LRET process.

transfer (LRET). LRET is generally more efficient than FRET, allowing for more effective excitation of the photosensitizers. While UC nanoparticles offer enormous potentials as light transducers for PDT, there still remain several issues that need to be addressed before they could be of practical use in clinical settings. The PDT effects were mostly examined *in vitro* and roughly estimated by measuring the generation of $^1O_2$. This could be partly attributed to the challenge in preparing ultrasmall (<10 nm) nanoparticles with well-defined surface properties and high UC efficiency. The capacity to load photosensitizers onto the UC nanoparticles without significantly increasing the particle size would greatly broaden the PDT application of these particles for *in vivo* studies.

6. Carbon-based nanomaterials

Carbon-based nanomaterials in forms of fullerenes, nanotubes and nanodiamonds exhibit a staggering variety of physical and chemical properties. As-produced crystalline forms of these nanomaterials are generally insoluble in most organic and aqueous solvent. However, upon surface engineering, for example, with hydrophilic moieties and cell receptor-binding ligands, they present new opportunities for targeted therapeutic applications.

6.1 Carbon fullerenes

Fullerenes are hollow and made entirely of surface carbon atoms. The cage-like structure of fullerenes has potential for use in clinical neuroscience. Fullerenes can act as potent neuroprotective agents that scavenge the free radicals associated with neurological disorders. Carboxylic acid-functionalized fullerene derivatives possess the ability to enter lipid membranes and inhibit cell death from oxidative stress. In recent years, fullerenes have also shown great potential as therapeutic agents in the prevention and treatment of Parkinson's disease. In addition to preventing neurological disorders, metallofullerenes can also function as drug carriers to target the delivery of anticancer drugs. Liang *et al.*[254] have shown that hydroxylated metallofullerene particles can cause accumulation of intracellular cisplatin drug in the CP-r cells, allowing for enhanced treatment of cancer with cisplatin both *in vitro* and *in vivo*.

6.2 Carbon nanotubes

The application of carbon nanotubes in therapeutics is not a trivial pursuit. This topic has been thoroughly reviewed by a several research groups.[255,256] The major factors that have driven the utility of carbon nanotubes in the therapeutic applications described here are their unique surface, electrical, mechanical and thermal properties in the context of the physiological environment. For example, depending on size and shape, these tubular forms of carbon can display a range of different conducting properties from metallic to semiconducting. They also have high drug loading capacities and good cell penetration capabilities. They can be made water dispersible either through non-covalent coating with amphiphilic macromolecules or through covalent functionalization by cycloaddition.

Covalently functionalized carbon nanotubes are reportedly nontoxic to cells and able to translocate directly into the cytoplasm of different types of cells.[257] These nanotubes have been investigated in drug and gene delivery for cancer treatment, typified by the anticancer drug cisplatin, palcitaxel and gene silencing siRNA molecules. Representative examples include the work of Bhirde *et al.*,[258] which shows the targeted killing of head and neck squamous cancer cells by using epidermal growth factor-modified carbon nanotubes, and the work of Dhar *et al.*,[259] which demonstrates the delivery of the cisplatin-loaded carbon nanotubes with targeting folate moiety to human choriocarcinoma and nasopharyngeal carcinoma cells.

The ability of carbon nanotubes to absorb NIR irradiation (700–1100 nm) and convert it into heat enables the exploitation of their use in thermal ablation application. Marches *et al.*[260] have demonstrated specific thermal ablation of human B lymphoma cells by using carbon nanotubes. The nanotubes were modified with CD22 antibodies that specifically target the lymphoma cells. When compared with the unmodified nanotubes, the viability of the cells pretreated with antibody-modified nanotubes was significantly reduced following exposure to NIR light. In a recent study, Choi and co-workers[261] have taken one step further and demonstrated the use of carbon nanotube-mediated thermal ablation for removing malignant tumors in living mice (Fig. 27). Upon NIR irradiation to the tumor region where PEG-modified single-walled carbon nanotubes were intratumorally injected, complete destruction of the tumors were observed without notable side effects or recurrence of tumors over 6 months. Their studies also suggested that most of injected carbon nanotubes were excreted from the body after 2 months through the biliary or urinary pathway.

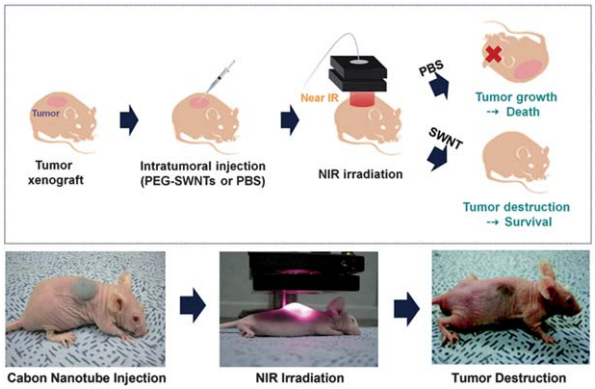

Fig. 27 Schematic showing the process of photothermal treatment through use of PEG-modified carbon nanotubes for a living mouse with a solid tumor on its back. (Reprinted with permission from ref. 261. Copyright 2009, American Chemical Society.)

6.3 Nanodiamonds

Over the past five years, there has been a surge of interest in developing diamond nanoparticles for therapeutic applications. These nanodiamonds, approximately 2 to 8 nm in diameter, have shown excellent biocompatibility and interesting luminescence properties.[262,263] These relevant characteristics can be harnessed to develop novel schemes of drug and gene delivery with high efficiency. For example, Ho and co-workers[264,265] have shown that nanodiamonds functionalized with polyethyleneimine (PEI800) are able to bind DNA plasmids and deliver them into mammalian cells. In fact, the transfection efficiency is much greater for these nanoconjugates than PEI800 alone. Building on these results, these researchers have recently demonstrated the delivery of doxorubicin drug to mice for the treatment of liver and breast cancer. With the assistance of nanodiamonds, significantly increased apoptosis and tumor growth inhibition were observed beyond the effect of conventional doxorubicin chemotherapy. It is apparent that the unique properties of nanodiamonds have enabled their use in advanced therapeutics, despite the need of improvements in the cellular and the subcellular targeting of the diamond nanoparticles.

7. Conclusion and prospects

Recent advances in nanoparticle engineering suggest that functional nanomaterials have the power to transform health care within the foreseeable future. The laborious process of conventional therapeutics can be made orders of magnitude more efficient through utilization of systems with defined structures and function at the nanometer scale. Complementary to conventional polymer-based delivery methods, the techniques described above are able to facilitate the delivery of drug molecules with high efficacy, while offering greater specificity for the treatment of diseases such as cancer. The inherent properties of functional materials in response to external stimulus manipulation to deliver drugs or directly provide therapeutic interventions would significantly improve drug formulations for existing therapies with fewer or reduced side effects.

The challenge for the future is to stimulate innovations based on material and structural designs that offer controlled release systems incorporating multiple drugs. New technologies need to be developed to derive a detailed understanding of how human cells interact with some specific types of nanomaterials within the context of a three-dimensional environment. Coordinated efforts from the nanotechnology, biomedical and clinical communities are also required to establish protocols for the selection of the most effective therapeutic approach.

Acknowledgements

X. L. acknowledges the Singapore–Peking–Oxford Research Enterprise (SPORE), the Singapore-MIT Alliance, the Ministry of Eduction, and the Agency for Science, Technology and Research (A*STAR) for supporting this work.

References

1 H. Jatzkewitz, *Z. Naturforsch., Teil B*, 1955, **10**, 27–31.
2 H. Brem, S. Piantadosi, P. C. Burger, M. Walker, R. Selker, N. A. Vick, K. Black, M. Sisti, S. Brem, G. Mohr, P. Muller, R. Morawetz and S. C. Schold, *Lancet*, 1995, **345**, 1008–1012.
3 R. A. Petros and J. M. DeSimone, *Nat. Rev. Drug Discovery*, 2010, **9**, 615–627.
4 M. E. Davis, Z. Chen and D. M. Shin, *Nat. Rev. Drug Discovery*, 2008, **7**, 771–782.
5 E. Boisselier and D. Astruc, *Chem. Soc. Rev.*, 2009, **38**, 1759–1782.
6 C. K. Kim, P. Ghosh and V. M. Rotello, *Nanoscale*, 2009, **1**, 61–67.
7 K. Park, S. Lee, E. Kang, K. Kim, K. Choi and I. C. Kwon, *Adv. Funct. Mater.*, 2009, **19**, 1553–1566.
8 K. T. Yong, I. Roy, M. T. Swihart and P. N. Prasad, *J. Mater. Chem.*, 2009, **19**, 4655–4672.
9 L. L. Dugan, D. M. Turetsky, C. Du, D. Lobner, M. Wheeler, C. R. Almli, C. K. F. Shen, T. Y. Luh, D. W. Choi and T. S. Lin, *Proc. Natl. Acad. Sci. U. S. A.*, 1997, **94**, 9434–9439.
10 R. Hao, R. Xing, Z. Xu, Y. Hou, S. Gao and S. Sun, *Adv. Mater.*, 2010, **22**, 2729–2742.
11 W. C. W. Chan, D. J. Maxwell, X. H. Gao, R. E. Bailey, M. Y. Han and S. M. Nie, *Curr. Opin. Biotechnol.*, 2002, **13**, 40–46.
12 F. Wang, D. Banerjee, Y. Liu, X. Chen and X. Liu, *Analyst*, 2010, **135**, 1839–1854.
13 R. Jin, Y. Cao, C. A. Mirkin, K. L. Kelly, G. C. Schatz and J. G. Zheng, *Science*, 2001, **294**, 1901–1903.
14 M. Y. Han, X. H. Gao, J. Z. Su and S. Nie, *Nat. Biotechnol.*, 2001, **19**, 631–635.
15 F. Wang and X. G. Liu, *J. Am. Chem. Soc.*, 2008, **130**, 5642–5643.
16 S. L. Zhang, J. Li, G. Lykotrafitis, G. Bao and S. Suresh, *Adv. Mater.*, 2009, **21**, 419–424.
17 M. R. Dreher, W. Liu, C. R. Michelich, M. W. Dewhirst, F. Yuan and A. Chilkoti, *J. Natl. Cancer Inst.*, 2006, **98**, 335–344.
18 P. Jani, G. W. Halbert, J. Langridge and A. T. Florence, *J. Pharm. Pharmacol.*, 1990, **42**, 821–826.
19 F. M. Henretig and A. R. Temple, *Clin. Lab. Med.*, 1984, **4**, 575–586.
20 Y. Cheng, J. D. Meyers, A.-M. Broome, M. E. Kenney, J. P. Basilion and C. Burda, *J. Am. Chem. Soc.*, 2011, **133**, 2583–2591.
21 N. L. Rosi and C. A. Mirkin, *Chem. Rev.*, 2005, **105**, 1547–1562.
22 F. Wang and X. G. Liu, *Chem. Soc. Rev.*, 2009, **38**, 976–989.
23 E. Tasciotti, X. W. Liu, R. Bhavane, K. Plant, A. D. Leonard, B. K. Price, M. M. C. Cheng, P. Decuzzi, J. M. Tour, F. Robertson and M. Ferrari, *Nat. Nanotechnol.*, 2008, **3**, 151–157.
24 F. M. Kievit, O. Veiseh, N. Bhattarai, C. Fang, J. W. Gunn, D. Lee, R. G. Ellenbogen, J. M. Olson and M. Q. Zhang, *Adv. Funct. Mater.*, 2009, **19**, 2244–2251.
25 J. M. Rosenholm, A. Meinander, E. Peulhu, R. Niemi, J. E. Eriksson, C. Sahlgren and M. Linden, *ACS Nano*, 2009, **3**, 197–206.
26 J. H. Park, L. Gu, G. von Maltzahn, E. Ruoslahti, S. N. Bhatia and M. J. Sailor, *Nat. Mater.*, 2009, **8**, 331–336.
27 W. C. W. Chan and S. M. Nie, *Science*, 1998, **281**, 2016–2018.
28 A. Sood and R. Panchagnula, *Chem. Rev.*, 2001, **101**, 3275–3304.
29 N. A. Monteiro-Riviere and J. E. Riviere, *Nanotoxicology*, 2009, **3**, 188–193.
30 J. S. Patton and P. R. Byron, *Nat. Rev. Drug Discovery*, 2007, **6**, 67–74.
31 U. Pison, T. Welte, M. Giersig and D. A. Groneberg, *Eur. J. Pharmacol.*, 2006, **533**, 341–350.
32 P. Nativo, I. A. Prior and M. Brust, *ACS Nano*, 2008, **2**, 1639–1644.
33 A. Mitra, J. Mulholland, A. Nan, E. McNeill, H. Ghandehari and B. R. Line, *J. Controlled Release*, 2005, **102**, 191–201.
34 D. Pissuwan, S. M. Valenzuela and M. B. Cortie, *Trends Biotechnol.*, 2006, **24**, 62–67.
35 D. Pissuwan, S. M. Valenzuela, C. M. Miller, M. C. Killingsworth and M. B. Cortie, *Small*, 2009, **5**, 1030–1034.
36 E. Y. Lukianova-Hleb, E. Y. Hanna, J. H. Hafner and D. O. Lapotko, *Nanotechnology*, 2010, **21**, 085102.
37 C. Park, H. Youn, H. Kim, T. Noh, Y. H. Kook, E. T. Oh, H. J. Park and C. Kim, *J. Mater. Chem.*, 2009, **19**, 2310–2315.
38 S. Dhar, W. L. Daniel, D. A. Giljohann, C. A. Mirkin and S. J. Lippard, *J. Am. Chem. Soc.*, 2009, **131**, 14652–14653.
39 J. S. Lee, J. J. Green, K. T. Love, J. Sunshine, R. Langer and D. G. Anderson, *Nano Lett.*, 2009, **9**, 2402–2406.
40 W. N. Rahman, N. Bishara, T. Ackerly, C. F. He, P. Jackson, C. Wong, R. Davidson and M. Geso, *Nanomed.: Nanotechnol., Biol. Med.*, 2009, **5**, 136–142.
41 C. H. J. Choi, C. A. Alabi, P. Webster and M. E. Davis, *Proc. Natl. Acad. Sci. U. S. A.*, 2009, **107**, 1235–1240.
42 X. H. Huang, I. H. El-Sayed, W. Qian and M. A. El-Sayed, *J. Am. Chem. Soc.*, 2006, **128**, 2115–2120.
43 F. Ratto, P. Matteini, F. Rossi, L. Menabuoni, N. Tiwari, S. K. Kulkarni and R. Pini, *Nanomed.: Nanotechnol., Biol. Med.*, 2009, **5**, 143–151.
44 A. Wijaya, S. B. Schaffer, I. G. Pallares and K. Hamad-Schifferli, *ACS Nano*, 2009, **3**, 80–86.
45 J. H. Park, G. von Maltzahn, L. L. Ong, A. Centrone, T. A. Hatton, E. Ruoslahti, S. N. Bhatia and M. J. Sailor, *Adv. Mater.*, 2010, **22**, 880–885.
46 L. R. Bickford, G. Agollah, R. Drezek and T. K. Yu, *Breast Cancer Res. Treat.*, 2009, **120**, 547–555.
47 T. S. Troutman, S. J. Leung and M. Romanowski, *Adv. Mater.*, 2009, **21**, 2334–2338.
48 J. You, G. D. Zhang and C. Li, *ACS Nano*, 2010, **4**, 1033–1041.
49 X. Wu, T. Ming, X. Wang, P. N. Wang, J. F. Wang and J. Y. Chen, *ACS Nano*, 2010, **4**, 113–120.
50 M. P. Melancon, W. Lu, Z. Yang, R. Zhang, Z. Cheng, A. M. Elliot, J. Stafford, T. Olson, J. Z. Zhang and C. Li, *Mol. Cancer Ther.*, 2008, **7**, 1730–1739.
51 W. Lu, C. Xiong, G. Zhang, Q. Huang, R. Zhang, J. Z. Zhang and C. Li, *Clin. Cancer Res.*, 2009, **15**, 876–886.
52 K. C. Grabar, R. G. Freeman, M. B. Hommer and M. J. Natan, *Anal. Chem.*, 1995, **67**, 735–743.
53 J. W. Liu, Z. H. Cao and Y. Lu, *Chem. Rev.*, 2009, **109**, 1948–1998.
54 J. H. Lee, M. V. Yigit, D. Mazumdar and Y. Lu, *Adv. Drug Delivery Rev.*, 2010, **62**, 592–605.
55 D. Li, S. P. Song and C. H. Fan, *Acc. Chem. Res.*, 2010, **43**, 631–641.
56 H. J. Zhang, R. J. Barsotti, C. L. Wong, X. J. Xue, X. G. Liu, F. Stellacci and J. T. L. Thong, *Small*, 2009, **5**, 2797–2801.

57 X. J. Xue, W. Xu, F. Wang and X. G. Liu, *J. Am. Chem. Soc.*, 2009, **131**, 11668–11669.
58 X. J. Xue, F. Wang and X. G. Liu, *J. Am. Chem. Soc.*, 2008, **130**, 3244–3245.
59 W. Xu, X. J. Xue, T. H. Li, H. Q. Zeng and X. G. Liu, *Angew. Chem., Int. Ed.*, 2009, **48**, 6849–6852.
60 X. Xie, W. Xu, T. Li and X. Liu, *Small*, 2011, **7**, 1393.
61 H. J. Zhang, W. Xu, X. G. Liu, F. Stellacci and J. T. L. Thong, *Appl. Phys. Lett.*, 2010, **97**, 163702.
62 Y. N. Tan, X. D. Su, Y. Zhu and J. Y. Lee, *ACS Nano*, 2010, **4**, 5101–5110.
63 Y. N. Tan, X. D. Su, E. T. Liu and J. S. Thomsen, *Anal. Chem.*, 2010, **82**, 2759–2765.
64 J. Nam, N. Won, H. Jin, H. Chung and S. Kim, *J. Am. Chem. Soc.*, 2009, **131**, 13639–13645.
65 S. S. Agasti, A. Chompoosor, C. C. You, P. Ghosh, C. K. Kim and V. M. Rotello, *J. Am. Chem. Soc.*, 2009, **131**, 5728–5729.
66 C. R. Patra, R. Bhattacharya and P. Mukherjee, *J. Mater. Chem.*, 2010, **20**, 547–554.
67 S. Aryal, J. J. Grailer, S. Pilla, D. A. Steeber and S. Q. Gong, *J. Mater. Chem.*, 2009, **19**, 7879–7884.
68 D. A. Giljohann, D. S. Seferos, A. E. Prigodich, P. C. Patel and C. A. Mirkin, *J. Am. Chem. Soc.*, 2009, **131**, 2072–2073.
69 B. Kang, M. A. Mackey and M. A. El-Sayed, *J. Am. Chem. Soc.*, 2010, **132**, 1517–1518.
70 A. Verma, O. Uzun, Y. H. Hu, Y. Hu, H. S. Han, N. Watson, S. L. Chen, D. J. Irvine and F. Stellacci, *Nat. Mater.*, 2008, **7**, 588–595.
71 R. Weissleder, *Nat. Biotechnol.*, 2001, **19**, 316–317.
72 Y. F. Huang, K. Sefah, S. Bamrungsap, H. T. Chang and W. Tan, *Langmuir*, 2008, **24**, 11860–11865.
73 K. V. Chakravarthy, A. C. Bonoiu, W. G. Davis, P. Ranjan, H. Ding, R. Hu, J. B. Bowzard, E. J. Bergey, J. M. Katz, P. R. Knight, S. Sambhara and P. N. Prasad, *Proc. Natl. Acad. Sci. U. S. A.*, 2010, **107**, 10172–10177.
74 A. M. Schwartzberg, T. Y. Olson, C. E. Talley and J. Z. Zhang, *J. Phys. Chem. B*, 2006, **110**, 19935–19944.
75 J. Z. Zhang, *J. Phys. Chem. Lett.*, 2010, **1**, 686–695.
76 L. R. Hirsch, R. J. Stafford, J. A. Bankson, S. R. Sershen, B. Rivera, R. E. Price, J. D. Hazle, N. J. Halas and J. L. West, *Proc. Natl. Acad. Sci. U. S. A.*, 2003, **100**, 13549–13554.
77 A. B. S. Bakhtiari, D. Hsiao, G. X. Jin, B. D. Gates and N. R. Branda, *Angew. Chem., Int. Ed.*, 2009, **48**, 4166–4169.
78 J. Yang, J. Lee, J. Kang, S. J. Oh, H. J. Ko, J. H. Son, K. Lee, J. S. Suh, Y. M. Huh and S. Haam, *Adv. Mater.*, 2009, **21**, 4339–4342.
79 H. Park, J. Yang, J. Lee, S. Haam, I. H. Choi and K. H. Yoo, *ACS Nano*, 2009, **3**, 2919–2926.
80 J. W. Kim, E. I. Galanzha, E. V. Shashkov, H. M. Moon and V. P. Zharov, *Nat. Nanotechnol.*, 2009, **4**, 688–694.
81 Y. Lu, Y. Zhao, L. Yu, L. Dong, C. Shi, M. J. Hu, Y. J. Xu, L. P. Wen and S. H. Yu, *Adv. Mater.*, 2010, **22**, 1407–1411.
82 J. Lee, J. Yang, H. Ko, S. J. Oh, J. Kang, J. H. Son, K. Lee, S. W. Lee, H. G. Yoon, J. S. Suh, Y. M. Huh and S. Haam, *Adv. Funct. Mater.*, 2008, **18**, 258–264.
83 X. Ji, R. Shao, A. M. Elliott, R. J. Stafford, E. Esparza-Coss, J. A. Bankson, G. Liang, Z.-P. Luo, K. Park, J. T. Markert and C. Li, *J. Phys. Chem. C*, 2007, **111**, 6245–6251.
84 V. Salgueiriño-Maceira, M. A. Correa-Duarte, M. Farle, A. López-Quintela, K. Sieradzki and R. Diaz, *Chem. Mater.*, 2006, **18**, 2701–2706.
85 Y. Piao, J. Kim, H. B. Na, D. Kim, J. S. Baek, M. K. Ko, J. H. Lee, M. Shokouhimehr and T. Hyeon, *Nat. Mater.*, 2008, **7**, 242–247.
86 W. C. Huang, P. J. Tsai and Y. C. Chen, *Small*, 2009, **5**, 51–56.
87 Y. Jin, C. Jia, S.-W. Huang, M. O'Donnell and X. Gao, *Nat. Commun.*, 2010, **1**, 1.
88 F. Y. Cheng, C. T. Chen and C. S. Yeh, *Nanotechnology*, 2009, **20**, 425104.
89 S. Link and M. A. El-Sayed, *Int. Rev. Phys. Chem.*, 2000, **19**, 409–453.
90 G. von Maltzahn, J. H. Park, A. Agrawal, N. K. Bandaru, S. K. Das, M. J. Sailor and S. N. Bhatia, *Cancer Res.*, 2009, **69**, 3892–3900.
91 M. S. Yavuz, Y. Cheng, J. Chen, C. M. Cobley, Q. Zhang, M. Rycenga, J. Xie, C. Kim, K. H. Song, A. G. Schwartz, L. V. Wang and Y. Xia, *Nat. Mater.*, 2009, **8**, 935–939.
92 J. Chen, C. Glaus, R. Laforest, Q. Zhang, M. Yang, M. Gidding, M. J. Welch and Y. Xia, *Small*, 2010, **6**, 811–817.
93 S.-W. Choi, Y. Zhang and Y. Xia, *Angew. Chem., Int. Ed.*, 2010, **49**, 7904–7908.
94 C. Fang and M. Q. Zhang, *J. Mater. Chem.*, 2009, **19**, 6258–6266.
95 J. R. McCarthy and R. Weissleder, *Adv. Drug Delivery Rev.*, 2008, **60**, 1241–1251.
96 T. K. Jain, M. A. Morales, S. K. Sahoo, D. L. Leslie-Pelecky and V. Labhasetwar, *Mol. Pharmaceutics*, 2005, **2**, 194–205.
97 H. Lee, M. K. Yu, S. Park, S. Moon, J. J. Min, Y. Y. Jeong, H. W. Kang and S. Jon, *J. Am. Chem. Soc.*, 2007, **129**, 12739–12745.
98 J. Zhang, S. Rana, R. S. Srivastava and R. D. K. Misra, *Acta Biomater.*, 2008, **4**, 40–48.
99 B. Julian-Lopez, C. Boissiere, C. Chaneac, D. Grosso, S. Vasseur, S. Miraux, E. Duguet and C. Sanchez, *J. Mater. Chem.*, 2007, **17**, 1563–1569.
100 N. Kawai, M. Futakuchi, T. Yoshida, A. Ito, S. Sato, T. Naiki, H. Honda, T. Shirai and K. Kohri, *Prostate*, 2008, **68**, 784–792.
101 P. Drake, H. J. Cho, P. S. Shih, C. H. Kao, K. F. Lee, C. H. Kuo, X. Z. Lin and Y. J. Lin, *J. Mater. Chem.*, 2007, **17**, 4914–4918.
102 C. R. De Silva, S. Smith, I. Shim, J. Pyun, T. Gutu, J. Jiao and Z. P. Zheng, *J. Am. Chem. Soc.*, 2009, **131**, 6336–6337.
103 S. H. Hu and X. H. Gao, *J. Am. Chem. Soc.*, 2010, **132**, 7234–7237.
104 R. John, R. Rezaeipoor, S. G. Adie, E. J. Chaney, A. L. Oldenburg, M. Marjanovic, J. P. Haldar, B. P. Sutton and S. A. Boppart, *Proc. Natl. Acad. Sci. U. S. A.*, 2010, **107**, 8085–8090.
105 M. Chorny, I. Fishbein, B. B. Yellen, I. S. Alferiev, M. Bakay, S. Ganta, R. Adamo, M. Amiji, G. Friedman and R. J. Levy, *Proc. Natl. Acad. Sci. U. S. A.*, 2010, **107**, 8346–8351.
106 J. E. Lee, N. Lee, H. Kim, J. Kim, S. H. Choi, J. H. Kim, T. Kim, I. C. Song, S. P. Park, W. K. Moon and T. Hyeon, *J. Am. Chem. Soc.*, 2010, **132**, 552–557.
107 K. El-Boubbou, D. C. Zhu, C. Vasileiou, B. Borhan, D. Prosperi, W. Li and X. F. Huang, *J. Am. Chem. Soc.*, 2010, **132**, 4490–4499.
108 C. R. Sun, K. Du, C. Fang, N. Bhattarai, O. Veiseh, F. Kievit, Z. Stephen, D. H. Lee, R. G. Ellenbogen, B. Ratner and M. Q. Zhang, *ACS Nano*, 2010, **4**, 2402–2410.
109 M. C. Franchini, G. Baldi, D. Bonacchi, D. Gentili, G. Giudetti, A. Lascialfari, M. Corti, P. Marmorato, J. Ponti, E. Micotti, U. Guerrini, L. Sironi, P. Gelosa, C. Ravagli and A. Ricci, *Small*, 2010, **6**, 366–370.
110 H. C. Wu, T. W. Wang, M. C. Bohn, F. H. Lin and M. Spector, *Adv. Funct. Mater.*, 2010, **20**, 67–77.
111 D. H. Kim, E. A. Rozhkova, I. V. Ulasov, S. D. Bader, T. Rajh, M. S. Lesniak and V. Novosad, *Nat. Mater.*, 2009, **9**, 165–171.
112 B. Thierry, F. Al-Ejeh, A. Khatri, Z. Yuan, P. J. Russell, S. Ping, M. P. Brown and P. Majewski, *Chem. Commun.*, 2009, 7348–7350.
113 C. J. Xu, Z. L. Yuan, N. Kohler, J. M. Kim, M. A. Chung and S. H. Sun, *J. Am. Chem. Soc.*, 2009, **131**, 15346–15351.
114 Y. Namiki, T. Namiki, H. Yoshida, Y. Ishii, A. Tsubota, S. Koido, K. Nariai, M. Mitsunaga, S. Yanagisawa, H. Kashiwagi, Y. Mabashi, Y. Yumoto, S. Hoshina, K. Fujise and N. Tada, *Nat. Nanotechnol.*, 2009, **4**, 598–606.
115 A. Hofmann, D. Wenzel, U. M. Becher, D. F. Freitag, A. M. Klein, D. Eberbeck, M. Schulte, K. Zimmermann, C. Bergemann, B. Gleich, W. Roell, T. Weyh, L. Trahms, G. Nickenig, B. K. Fleischmann and A. Pfeifer, *Proc. Natl. Acad. Sci. U. S. A.*, 2008, **106**, 44–49.
116 B. D. Wang, C. J. Xu, J. Xie, Z. Y. Yang and S. H. Sun, *J. Am. Chem. Soc.*, 2008, **130**, 14436–14437.
117 J. Kim, H. S. Kim, N. Lee, T. Kim, H. Kim, T. Yu, I. C. Song, W. K. Moon and T. Hyeon, *Angew. Chem., Int. Ed.*, 2008, **47**, 8438–8441.
118 M. Johannsen, U. Gneueckow, B. Thiesen, K. Taymoorian, C. H. Cho, N. Waldofner, R. Scholz, A. Jordan, S. A. Loening and P. Wust, *Eur. Urol.*, 2007, **52**, 1653–1662.
119 J. Xie, C. Xu, N. Kohler, Y. Hou and S. Sun, *Adv. Mater.*, 2007, **19**, 3163–3166.
120 W. S. Seo, J. H. Lee, X. M. Sun, Y. Suzuki, D. Mann, Z. Liu, M. Terashima, P. C. Yang, M. V. McConnell, D. G. Nishimura and H. J. Dai, *Nat. Mater.*, 2006, **5**, 971–976.
121 N. Kohler, C. Sun, A. Fichtenholtz, J. Gunn, C. Fang and M. Q. Zhang, *Small*, 2006, **2**, 785–792.
122 S. Mornet, S. Vasseur, F. Grasset and E. Duguet, *J. Mater. Chem.*, 2004, **14**, 2161–2175.

123 R. Hergt, S. Dutz, R. Muller and M. Zeisberger, *J. Phys.: Condens. Matter*, 2006, **18**, S2919–S2934.
124 C. C. Berry, *J. Mater. Chem.*, 2005, **15**, 543–547.
125 N. Kohler, C. Sun, J. Wang and M. Q. Zhang, *Langmuir*, 2005, **21**, 8858–8864.
126 C. Xu, B. Wang and S. Sun, *J. Am. Chem. Soc.*, 2009, **131**, 4216–4217.
127 F. Wang, W. B. Tan, Y. Zhang, X. P. Fan and M. Q. Wang, *Nanotechnology*, 2006, **17**, R1–R13.
128 J. Lee, G. D. Lilly, R. C. Doty, P. Podsiadlo and N. A. Kotov, *Small*, 2009, **5**, 1213–1221.
129 A. P. Alivisatos, *Science*, 1996, **271**, 933–937.
130 Q. Zhang, T. Sun, F. Cao, M. Li, M. Hong, J. Yuan, Q. Yan, H. H. Hng, N. Wu and X. Liu, *Nanoscale*, 2010, **2**, 1256–1259.
131 Y. He, H. Lu, Y. Su, L. Sai, M. Hu, C. Fan and L. Wang, *Biomaterials*, 2011, **32**, 2133–2140.
132 Y. He, H. T. Lu, L. M. Sai, W. Y. Lai, Q. L. Fan, L. H. Wang and W. Huang, *J. Phys. Chem. B*, 2006, **110**, 13352–13356.
133 Y. He, H. T. Lu, L. M. Sai, W. Y. Lai, Q. L. Fan, L. H. Wang and W. Huang, *J. Phys. Chem. B*, 2006, **110**, 13370–13374.
134 Y. He, H.-T. Lu, L.-M. Sai, Y.-Y. Su, M. Hu, C.-H. Fan, W. Huang and L.-H. Wang, *Adv. Mater.*, 2008, **20**, 3416–3421.
135 L. H. Yuwen, H. T. Lu, Y. He, L. Q. Chen, M. Hu, B. Q. Bao, F. Boey, H. Zhang and L. H. Wang, *J. Mater. Chem.*, 2010, **20**, 2788–2793.
136 Y. Su, M. Hu, C. Fan, Y. He, Q. Li, W. Li, L.-h. Wang, P. Shen and Q. Huang, *Biomaterials*, 2010, **31**, 4829–4834.
137 I. L. Medintz, H. T. Uyeda, E. R. Goldman and H. Mattoussi, *Nat. Mater.*, 2005, **4**, 435–446.
138 M. Bruchez Jr, M. Moronne, P. Gin, S. Weiss and A. P. Alivisatos, *Science*, 1998, **281**, 2013–2016.
139 M. E. Akerman, W. C. W. Chan, P. Laakkonen, S. N. Bhatia and E. Ruoslahti, *Proc. Natl. Acad. Sci. U. S. A.*, 2002, **99**, 12617–12621.
140 A. M. Derfus, W. C. W. Chan and S. N. Bhatia, *Adv. Mater.*, 2004, **16**, 961–966.
141 E. B. Voura, J. K. Jaiswal, H. Mattoussi and S. M. Simon, *Nat. Med.*, 2004, **10**, 993–998.
142 S. M. Nie, Y. Xing, G. J. Kim and J. W. Simons, *Annu. Rev. Biomed. Eng.*, 2007, **9**, 257–288.
143 H. Tada, H. Higuchi, T. M. Wanatabe and N. Ohuchi, *Cancer Res.*, 2007, **67**, 1138–1144.
144 J. H. Park, G. von Maltzahn, E. Ruoslahti, S. N. Bhatia and M. J. Sailor, *Angew. Chem., Int. Ed.*, 2008, **47**, 7284–7288.
145 M. V. Yezhelyev, L. F. Qi, R. M. O'Regan, S. Nie and X. H. Gao, *J. Am. Chem. Soc.*, 2008, **130**, 9006–9012.
146 H. S. Choi, W. Liu, F. Liu, K. Nasr, P. Misra, M. G. Bawendi and J. V. Frangioni, *Nat. Nanotechnol.*, 2009, **5**, 42–47.
147 X. H. Gao, Y. Y. Cui, R. M. Levenson, L. W. K. Chung and S. M. Nie, *Nat. Biotechnol.*, 2004, **22**, 969–976.
148 A. C. S. Samia, X. B. Chen and C. Burda, *J. Am. Chem. Soc.*, 2003, **125**, 15736–15737.
149 P. Juzenas, W. Chen, Y. P. Sun, M. A. N. Coelho, R. Generalov, N. Generalova and I. L. Christensen, *Adv. Drug Delivery Rev.*, 2008, **60**, 1600–1614.
150 V. Biju, S. Mundayoor, R. V. Omkumar, A. Anas and M. Ishikawa, *Biotechnol. Adv.*, 2010, **28**, 199–213.
151 R. Bakalova, H. Ohba, Z. Zhelev, M. Ishikawa and Y. Baba, *Nat. Biotechnol.*, 2004, **22**, 1360–1361.
152 A. Anas, H. Akita, H. Harashima, T. Itoh, M. Ishikawa and V. Biju, *J. Phys. Chem. B*, 2008, **112**, 10005–10011.
153 L. Yang, H. Mao, Y. A. Wang, Z. Cao, X. Peng, X. Wang, H. Duan, C. Ni, Q. Yuan, G. Adams, M. Q. Smith, W. C. Wood, X. Gao and S. Nie, *Small*, 2008, **5**, 235–243.
154 I. L. Medintz and H. Mattoussi, *Phys. Chem. Chem. Phys.*, 2009, **11**, 17–45.
155 X. Hu and X. Gao, *ACS Nano*, 2010, **4**, 6080–6086.
156 D. J. Bharali, D. W. Lucey, H. Jayakumar, H. E. Pudavar and P. N. Prasad, *J. Am. Chem. Soc.*, 2005, **127**, 11364–11371.
157 F. Vetrone and J. A. Capobianco, *Int. J. Nanotechnol.*, 2008, **5**, 1306–1339.
158 C. X. Li and J. Lin, *J. Mater. Chem.*, 2010, **20**, 6831–6847.
159 K. Binnemans, *Chem. Rev.*, 2009, **109**, 4283–4374.
160 S. V. Eliseeva and J. C. G. Bunzli, *Chem. Soc. Rev.*, 2010, **39**, 189–227.
161 J. Shen, L. D. Sun and C. H. Yan, *Dalton Trans.*, 2008, 5687–5697.
162 W. Q. Luo, R. F. Li and X. Y. Chen, *J. Phys. Chem. C*, 2009, **113**, 8772–8777.
163 F. Wang, X. P. Fan, M. Q. Wang and Y. Zhang, *Nanotechnology*, 2007, **18**, 025701.
164 F. Wang, J. Wang, J. Xu, X. J. Xue and X. G. Liu, *Spectrosc. Lett.*, 2010, **43**, 400–405.
165 F. Wang, X. J. Xue and X. G. Liu, *Angew. Chem., Int. Ed.*, 2008, **47**, 906–909.
166 O. Ehlert, R. Thomann, M. Darbandi and T. Nann, *ACS Nano*, 2008, **2**, 120–124.
167 J. Wang, F. Wang, J. Xu, Y. Wang, Y. Liu, X. Chen, H. Chen and X. Liu, *C. R. Chim.*, 2010, **13**, 731–736.
168 C. Jiang, F. Wang, N. Wu and X. Liu, *Adv. Mater.*, 2008, **20**, 4826–4829.
169 R. Sivakumar, F. van Veggel and M. Raudsepp, *J. Am. Chem. Soc.*, 2005, **127**, 12464–12465.
170 Y. Zhang, J. H. Hao, C. L. Mak and X. H. Wei, *Opt. Express*, 2011, **19**, 1824–1829.
171 H. T. Wong, H. L. W. Chan and J. H. Hao, *Opt. Express*, 2010, **18**, 6123–6130.
172 H. Zheng, X. J. X.-j. Wang, M. J. Dejneka, W. M. Yen and R. S. Meltzer, *J. Lumin.*, 2004, **108**, 395–399.
173 H. Zhang, Y. J. Li, Y. C. Lin, Y. Huang and X. F. Duan, *Nanoscale*, 2011, **3**, 963–966.
174 E. Beaurepaire, V. Buissette, M. P. Sauviat, D. Giaume, K. Lahlil, A. Mercuri, D. Casanova, A. Huignard, J. L. Martin, T. Gacoin, J. P. Boilot and A. Alexandrou, *Nano Lett.*, 2004, **4**, 2079–2083.
175 F. Auzel, *Chem. Rev.*, 2004, **104**, 139–173.
176 J. F. Suyver, A. Aebischer, D. Biner, P. Gerner, J. Grimm, S. Heer, K. W. Krämer, C. Reinhard and H. U. Güdel, *Opt. Mater.*, 2005, **27**, 1111–1130.
177 H. S. Mader, P. Kele, S. M. Saleh and O. S. Wolfbeis, *Curr. Opin. Chem. Biol.*, 2010, **14**, 582–596.
178 D. K. Chatterjee, M. K. Gnanasammandhan and Y. Zhang, *Small*, 2010, **6**, 2781–2795.
179 X. C. Ye, J. E. Collins, Y. J. Kang, J. Chen, D. T. N. Chen, A. G. Yodh and C. B. Murray, *Proc. Natl. Acad. Sci. U. S. A.*, 2010, **107**, 22430–22435.
180 G. F. Wang, W. P. Qin, G. D. Wei, L. L. Wang, P. F. Zhu, R. J. Kim, D. S. Zhang, F. H. Ding and K. Z. Zheng, *J. Fluorine Chem.*, 2009, **130**, 158–161.
181 B. Dong, H. W. Song, H. Q. Yu, H. Zhang, R. F. Qin, X. Bai, G. H. Pan, S. Z. Lu, F. Wang, L. B. Fan and Q. L. Dai, *J. Phys. Chem. C*, 2008, **112**, 1435–1440.
182 F. Wang, Y. Han, C. S. Lim, Y. H. Lu, J. Wang, J. Xu, H. Chen, C. Zhang, M. Hong and X. Liu, *Nature*, 2010, **463**, 1061–1065.
183 D. Q. Chen, Y. L. Yu, F. Huanga and Y. S. Wang, *Chem. Commun.*, 2011, **47**, 2601–2603.
184 S. Heer, O. Lehmann, M. Haase and H. U. Gudel, *Angew. Chem., Int. Ed.*, 2003, **42**, 3179–3182.
185 L. Y. Wang and Y. D. Li, *Chem. Mater.*, 2007, **19**, 727–734.
186 G. F. Wang, Q. Peng and Y. D. Li, *J. Am. Chem. Soc.*, 2009, **131**, 14200–14201.
187 H. X. Mai, Y. W. Zhang, R. Si, Z. G. Yan, L. D. Sun, L. P. You and C. H. Yan, *J. Am. Chem. Soc.*, 2006, **128**, 6426–6436.
188 G. S. Yi and G. M. Chow, *J. Mater. Chem.*, 2005, **15**, 4460–4464.
189 G. S. Yi, H. C. Lu, S. Y. Zhao, G. Yue, W. J. Yang, D. P. Chen and L. H. Guo, *Nano Lett.*, 2004, **4**, 2191–2196.
190 X. Wang, J. Zhuang, Q. Peng and Y. D. Li, *Nature*, 2005, **437**, 121–124.
191 D. L. Gao, H. R. Zheng, Y. Tian, M. Cui, Y. Lei, E. J. He and X. S. Zhang, *J. Nanosci. Nanotechnol.*, 2010, **10**, 7694–7697.
192 C. H. Liu, H. Wang, X. R. Zhang and D. P. Chen, *J. Mater. Chem.*, 2009, **19**, 489–496.
193 Z. W. Quan, P. P. Yang, C. X. Li, J. Yang, D. M. Yang, Y. Jin, H. Z. Lian, H. Y. Li and J. Lin, *J. Phys. Chem. C*, 2009, **113**, 4018–4025.
194 J. C. Boyer, L. A. Cuccia and J. A. Capobianco, *Nano Lett.*, 2007, **7**, 847–852.
195 J. C. Boyer, F. Vetrone, L. A. Cuccia and J. A. Capobianco, *J. Am. Chem. Soc.*, 2006, **128**, 7444–7445.
196 H. Q. Wang and T. Nann, *ACS Nano*, 2009, **3**, 3804–3808.
197 H. Schafer, P. Ptacek, K. Kompe and M. Haase, *Chem. Mater.*, 2007, **19**, 1396–1400.
198 H. Schafer, P. Ptacek, B. Voss, H. Eickmeier, J. Nordmann and M. Haase, *Cryst. Growth Des.*, 2010, **10**, 2202–2208.

199 H. Schafer, P. Ptacek, H. Eickmeier and M. Haase, *Adv. Funct. Mater.*, 2009, **19**, 3091–3097.
200 Z. L. Wang, J. H. Hao and H. L. W. Chan, *J. Mater. Chem.*, 2010, **20**, 3178–3185.
201 Z. L. Wang, J. H. Hao and H. L. W. Chan, *CrystEngComm*, 2010, **12**, 1373–1376.
202 X. Chen, W. J. Wang, X. Y. Chen, J. H. Bi, L. Wu, Z. H. Li and X. Z. Fu, *Mater. Lett.*, 2009, **63**, 1023–1026.
203 F. Wang, D. K. Chatterjee, Z. Q. Li, Y. Zhang, X. P. Fan and M. Q. Wang, *Nanotechnology*, 2006, **17**, 5786–5791.
204 C. K. Lin, M. T. Berry, R. Anderson, S. Smith and P. S. May, *Chem. Mater.*, 2009, **21**, 3406–3413.
205 X. F. Yu, M. Li, M. Y. Xie, L. D. Chen, Y. Li and Q. Q. Wang, *Nano Res.*, 2010, **3**, 51–60.
206 S. Zeng, G. Ren, C. Xu and Q. Yang, *CrystEngComm*, 2011, **13**, 4276.
207 D. Chen, Y. Yu, F. Huang, A. Yang and Y. Wang, *J. Mater. Chem.*, 2011, **21**, 6186–6192.
208 D. Q. Chen, Y. L. Yu, F. Huang, P. Huang, A. P. Yang and Y. S. Wang, *J. Am. Chem. Soc.*, 2010, **132**, 9976–9978.
209 H. X. Mai, Y. W. Zhang, L. D. Sun and C. H. Yan, *J. Phys. Chem. C*, 2007, **111**, 13721–13729.
210 F. Vetrone, R. Naccache, V. Mahalingam, C. G. Morgan and J. A. Capobianco, *Adv. Funct. Mater.*, 2009, **19**, 2924–2929.
211 G. S. Yi and G. M. Chow, *Chem. Mater.*, 2007, **19**, 341–343.
212 J. C. Boyer, M. P. Manseau, J. I. Murray and F. C. J. M. van Veggel, *Langmuir*, 2010, **26**, 1157–1164.
213 H. Schäfer, P. Ptacek, O. Zerzouf and M. Haase, *Adv. Funct. Mater.*, 2008, **18**, 2913–2918.
214 P. Ghosh, A. Kar and A. Patra, *Nanoscale*, 2010, **2**, 1196–1202.
215 H. Schafer, P. Ptacek, K. Hickmann, M. Prinz, M. Neumann and M. Haase, *Russ. J. Inorg. Chem.*, 2009, **54**, 1914–1920.
216 K. A. Abel, J. C. Boyer and F. C. J. M. van Veggel, *J. Am. Chem. Soc.*, 2009, **131**, 14644–14645.
217 F. Wang, J. Wang and X. G. Liu, *Angew. Chem., Int. Ed.*, 2010, **49**, 7456–7460.
218 W. Feng, L. D. Sun and C. H. Yan, *Chem. Commun.*, 2009, 4393–4395.
219 S. Schietinger, T. Aichele, H. Q. Wang, T. Nann and O. Benson, *Nano Lett.*, 2010, **10**, 134–138.
220 H. Zhang, Y. J. Li, I. A. Ivanov, Y. Q. Qu, Y. Huang and X. F. Duan, *Angew. Chem., Int. Ed.*, 2010, **49**, 2865–2868.
221 H. Zhang, D. Xu, Y. Huang and X. F. Duan, *Chem. Commun.*, 2011, **47**, 979–981.
222 H. Kobayashi, N. Kosaka, M. Ogawa, N. Y. Morgan, P. D. Smith, C. B. Murray, X. C. Ye, J. Collins, G. A. Kumar, H. Bell and P. L. Choyke, *J. Mater. Chem.*, 2009, **19**, 6481–6484.
223 L. A. Cheng, K. Yang, S. A. Zhang, M. W. Shao, S. T. Lee and Z. Liu, *Nano Res.*, 2010, **3**, 722–732.
224 D. E. Achatz, R. J. Meier, L. H. Fischer and O. S. Wolfbeis, *Angew. Chem., Int. Ed.*, 2011, **50**, 260–263.
225 H. H. Gorris, R. Ali, S. M. Saleh and O. S. Wolfbeis, *Adv. Mater.*, 2011, **23**, 1652–1655.
226 L.-N. Sun, H. Peng, M. I. J. Stich, D. Achatz and O. S. Wolfbeis, *Chem. Commun.*, 2009, 5000–5002.
227 T. Rantanen, M. L. Jarvenpaa, J. Vuojola, K. Kuningas and T. Soukka, *Angew. Chem., Int. Ed.*, 2008, **47**, 3811–3813.
228 T. Rentanen, M.-L. Järvenpää, J. Vuojola, R. Arppe, K. Kuningas and T. Soukka, *Analyst*, 2009, **134**, 1713–1716.
229 Y. I. Park, J. H. Kim, K. T. Lee, K.-S. Jeon, H. B. Na, J. H. Yu, H. M. Kin, N. Lee, S. H. Choi, S.-I. Baik, H. Kin, S. P. Park, B.-J. Park, Y. W. Kim, S. H. Lee, S.-Y. Yoon, I. C. Song, W. K. Moon, Y. D. Suh and T. Hyeon, *Adv. Mater.*, 2009, **21**, 4467–4471.
230 S. W. Wu, G. Han, D. J. Milliron, S. Aloni, V. Altoe, D. V. Talapin, B. E. Cohen and P. J. Schuck, *Proc. Natl. Acad. Sci. U. S. A.*, 2009, **106**, 10917–10921.
231 Z. Q. Li, Y. Zhang and S. Jiang, *Adv. Mater.*, 2008, **20**, 4765–4769.
232 J. N. Shan, J. B. Chen, J. Meng, J. Collins, W. Soboyejo, J. S. Friedberg and Y. G. Ju, *J. Appl. Phys.*, 2008, **104**, 094308.
233 G. K. Das, P. P. Y. Chan, A. Teo, J. S. C. Loo, J. M. Anderson and T. T. Y. Tan, *J. Biomed. Mater. Res., Part A*, 2010, **93**, 337–346.
234 F. Vetrone, R. Naccache, A. J. de la Fuente, F. Sanz-Rodriguez, A. Blazquez-Castro, E. M. Rodriguez, D. Jaque, J. G. Sole and J. A. Capobianco, *Nanoscale*, 2010, **2**, 495–498.
235 L. Qian, L. Zhou, H. P. Too and G. M. Chow, *J. Nanopart. Res.*, 2010, **13**, 499–510.
236 Z. L. Wang, J. Hao, H. L. W. Chan, G. L. Law, W. T. Wong, K. L. Wong, M. B. Murphy, T. Su, Z. H. Zhang and S. Q. Zeng, *Nanoscale*, 2011, **3**, 2175–2181.
237 J. Chen, C. R. Guo, M. Wang, L. Huang, L. P. Wang, C. C. Mi, J. Li, X. X. Fang, C. B. Mao and S. K. Xu, *J. Mater. Chem.*, 2011, **21**, 2632–2638.
238 T. Cao, Y. Yang, Y. Gao, J. Zhou, Z. Li and F. Li, *Biomaterials*, 2011, **32**, 2959–2968.
239 L. Xiong, T. Yang, Y. Yang, C. Xu and F. Li, *Biomaterials*, 2010, **31**, 7078–7085.
240 R. Kumar, M. Nyk, T. Y. Ohulchanskyy, C. A. Flask and P. N. Prasad, *Adv. Funct. Mater.*, 2009, **19**, 853–859.
241 J. Zhou, Y. Sun, X. Du, L. Xiong, H. Hu and F. Li, *Biomaterials*, 2010, **31**, 3287–3295.
242 J. Zhou, M. X. Yu, Y. Sun, X. Z. Zhang, X. J. Zhu, Z. H. Wu, D. M. Wu and F. Y. Li, *Biomaterials*, 2011, **32**, 1148–1156.
243 Q. Liu, Y. Sun, C. Li, J. Zhou, C. Li, T. Yang, X. Zhang, T. Yi, D. Wu and F. Li, *ACS Nano*, 2011, **5**, 3146–3157.
244 Z. H. Xu, C. X. Li, P. A. Ma, Z. Y. Hou, D. M. Yang, X. J. Kang and J. Lin, *Nanoscale*, 2011, **3**, 661–667.
245 Y. F. Yang, Y. Q. Qu, J. W. Zhao, Q. H. Zeng, Y. Y. Ran, Q. B. Zhang, X. G. Kong and H. Zhang, *Eur. J. Inorg. Chem.*, 2010, 5195–5199.
246 C. J. Carling, F. Nourmohammadian, J. C. Boyer and N. R. Branda, *Angew. Chem., Int. Ed.*, 2010, **49**, 3782–3785.
247 C. J. Carling, J. C. Boyer and N. R. Branda, *J. Am. Chem. Soc.*, 2009, **131**, 10838–10839.
248 C. D. S. Brites, P. P. Lima, N. J. O. Silva, A. Millan, V. S. Amaral, F. Palacio and L. D. Carlos, *New J. Chem.*, 2011, **35**, 1177.
249 L. Aigouy, E. Saidi, L. Lalouat, J. Labeguerie-Egea, M. Mortier, P. Low and C. Bergaud, *J. Appl. Phys.*, 2009, **106**, 074301.
250 F. Vetrone, R. Naccache, A. Zamarron, A. J. de la Fuente, F. Sanz-Rodriguez, L. M. Maestro, E. M. Rodriguez, D. Jaque, J. G. Sole and J. A. Capobianco, *ACS Nano*, 2010, **4**, 3254–3258.
251 P. Zhang, W. Steelant, M. Kumar and M. Scholfield, *J. Am. Chem. Soc.*, 2007, **129**, 4526–4527.
252 H. S. Qian, H. C. Guo, P. C. L. Ho, R. Mahendran and Y. Zhang, *Small*, 2009, **5**, 2285–2290.
253 B. Ungun, R. K. Prud'homme, S. J. Budijono, J. N. Shan, S. F. Lim, Y. G. Ju and R. Austin, *Opt. Express*, 2008, **17**, 80–86.
254 X. J. Liang, H. Meng, Y. Z. Wang, H. Y. He, J. Meng, J. Lu, P. C. Wang, Y. L. Zhao, X. Y. Gao, B. Y. Sun, C. Y. Chen, G. M. Xing, D. W. Shen, M. M. Gottesman, Y. Wu, J. J. Yin and L. Jia, *Proc. Natl. Acad. Sci. U. S. A.*, 2010, **107**, 7449–7454.
255 L. Lacerda, A. Bianco, M. Prato and K. Kostarelos, *Adv. Drug Delivery Rev.*, 2006, **58**, 1460–1470.
256 T. A. Hilder and J. M. Hill, *Small*, 2009, **5**, 300–308.
257 K. Kostarelos, L. Lacerda, G. Pastorin, W. Wu, S. Wieckowski, J. Luangsivilay, S. Godefroy, D. Pantarotto, J. P. Briand, S. Muller, M. Prato and A. Bianco, *Nat. Nanotechnol.*, 2007, **2**, 108–113.
258 A. A. Bhirde, V. Patel, J. Gavard, G. F. Zhang, A. A. Sousa, A. Masedunskas, R. D. Leapman, R. Weigert, J. S. Gutkind and J. F. Rusling, *ACS Nano*, 2009, **3**, 307–316.
259 S. Dhar, Z. Liu, J. Thomale, H. J. Dai and S. J. Lippard, *J. Am. Chem. Soc.*, 2008, **130**, 11467–11476.
260 R. Marches, P. Chakravarty, I. H. Musselman, P. Bajaj, R. N. Azad, P. Pantano, R. K. Draper and E. S. Vitetta, *Int. J. Cancer*, 2009, **125**, 2970–2977.
261 H. K. Moon, S. H. Lee and H. C. Choi, *ACS Nano*, 2009, **3**, 3707–3713.
262 Y. L. Zhong, K. F. Chong, P. W. May, Z.-K. Chen and K. P. Loh, *Langmuir*, 2007, **23**, 5824–5830.
263 W. S. Yeap, Y. Y. Tan and K. P. Loh, *Anal. Chem.*, 2008, **80**, 4659–4665.
264 E. K. Chow, X.-Q. Zhang, M. Chen, R. Lam, E. Robinson, H. Huang, D. Schaffer, E. Osawa, A. Goga and D. Ho, *Sci. Transl. Med.*, 2011, **3**, 73ra21.
265 M. Chen, E. D. Pierstorff, R. Lam, S. Y. Li, H. Huang, E. Osawa and D. Ho, *ACS Nano*, 2009, **3**, 2016–2022.